On discrete Lorenz-like attractors

Cite as: Chaos **31**, 023117 (2021); https://doi.org/10.1063/5.0037621
Submitted: 14 November 2020 . Accepted: 20 January 2021 . Published Online: 10 February 2021

Sergey Gonchenko, Alexander Gonchenko, Alexey Kazakov, and Evgeniya Samylina

On discrete Lorenz-like attractors

Cite as: Chaos **31**, 023117 (2021); doi: 10.1063/5.0037621
Submitted: 14 November 2020 · Accepted: 20 January 2021 ·
Published Online: 10 February 2021

Sergey Gonchenko,[1,a)] Alexander Gonchenko,[1] Alexey Kazakov,[2] and Evgeniya Samylina[2]

AFFILIATIONS

[1]Mathematical Center of Lobachevsky State University, 23 Prospekt Gagarina, 603950 Nizhny Novgorod, Russia
[2]National Research University Higher School of Economics, 25/12 Bolshaya Pecherskaya Ulitsa, 603155 Nizhny Novgorod, Russia

Note: This paper is part of the Focus Issue, Global Bifurcations, Chaos, and Hyperchaos: Theory and Applications.
[a)]**Author to whom correspondence should be addressed:** sergey.gonchenko@mail.ru

ABSTRACT

We study geometrical and dynamical properties of the so-called discrete Lorenz-like attractors. We show that such robustly chaotic (pseudohyperbolic) attractors can appear as a result of universal bifurcation scenarios, for which we give a phenomenological description and demonstrate certain examples of their implementation in one-parameter families of three-dimensional Hénon-like maps. We pay special attention to such scenarios that can lead to period-2 Lorenz-like attractors. These attractors have very interesting dynamical properties and we show that their crises can lead, in turn, to the emergence of discrete Lorenz shape attractors of new types.

The topic related to the study of the Lorenz attractors has always been a priority for Shilnikov. The results obtained in this area by himself and his co-authors, including the famous Afraimovich–Bykov–Shilnikov geometrical model,[1,2] constitute the foundation of the theory of the Lorenz attractors. The present paper can be viewed in the context of the development of this theory but already for the so-called discrete Lorenz-like attractors of three-dimensional maps. Such attractors were discovered in Ref. 3. In the current study, we describe the main properties of various types of discrete Lorenz-like attractors of three-dimensional maps, paying special attention to both bifurcation scenarios of their appearance and properties of robustness (pseudohyperbolicity) of its chaotic dynamics. Among the obtained results, we would like to mention the following ones: (i) new realistic scenarios of the appearance of the discrete Lorenz-like attractors and examples of their implementation in one-parameter families of three-dimensional maps; (ii) discrete Lorenz-like attractors of principally new types (period-2 homoclinic and heteroclinic such attractors); and (iii) the numerical evidence of pseudohyperbolicity for attractors under consideration.

I. INTRODUCTION

In the theory of dynamical chaos, problems related to the study of strange attractors of multidimensional systems (with a dimension of phase space ≥ 4 for flows and ≥ 3 for diffeomorphisms) are among the most important and interesting ones. Naturally, the solution to these problems should be based on fundamental results obtained in the theory of chaos in smaller dimensions. First, the results that are associated with the discovery of the Lorenz attractor[4] and the creation of its mathematical models,[1,2,5] as well as with the proof of its robust chaoticity, should be noted.[6–9] These results, as well as studies on Hénon-like attractors of two-dimensional diffeomorphisms,[10–14] served as a kind of foundation on which the basic elements of the theory of strange attractors of three-dimensional maps were built.[3,15–20]

Recall that a strange attractor of a diffeomorphism is called *discrete homoclinic attractor*[17] if it contains only one fixed point, a hyperbolic saddle, and entirely its unstable invariant manifold that possesses transversal homoclinic points (points where stable and unstable manifolds of the saddle intersect transversally). In the case of two-dimensional maps, examples of discrete homoclinic attractors are well known: for example, there are the above Hénon-like attractors and attractors in periodically perturbed systems with a homoclinic figure-8 of a saddle, or attractors in the corresponding double separatrix maps (see Ref. 21).

In the present study, we consider three-dimensional diffeomorphisms which, on the one hand, are an independent subject of the theory of dynamical systems and, on the other hand, can be represented as Poincaré maps of four-dimensional flows or, when the diffeomorphism is nonorientable (its Jacobian is negative at all points of the phase space), as a model for studying Poincaré maps of five-dimensional flows.

The first explicit examples of discrete homoclinic attractors in the case of three-dimensional diffeomorphisms were given in Ref. 3, in which they were found in three-dimensional maps of the form

$$\bar{x} = y, \quad \bar{y} = z, \quad \bar{z} = M_1 + Bx + M_2 y - z^2, \tag{1}$$

where M_1, M_2, and B are parameters, and B is the Jacobian of map (1). Note that map (1) is a three-dimensional extension for the standard Hénon map $\bar{y} = z$, and $\bar{z} = M_1 + M_2 y - z^2$ (the latter is obtained at $B = 0$, when the coordinate x is separated); therefore, we will call map (1) the *three-dimensional Hénon map*.

In Fig. 1, phase portraits of some attractors of map (1) (based on Ref. 3) are shown. The first two examples, shown in Figs. 1(a) and 1(b), relate to discrete homoclinic attractors [containing a saddle fixed point $O(x = y = z = B + M_2 - 1)$] that are very similar to the classical Lorenz attractor.[4]

More informally, we define a *discrete Lorenz-like attractor A* as follows:

(i) A is a homoclinic attractor containing a saddle fixed point O with eigenvalues $\gamma, \lambda_1, \lambda_2$ such that $|\gamma| > 1, 0 < |\lambda_2| < \lambda_1 < 1$, $|\lambda_1 \lambda_2 \gamma| < 1$, and $\sigma \equiv |\lambda_1 \gamma| > 1$;
(ii) let Γ_1 and Γ_2 be the unstable separatrices of O, i.e., connected components of the set $W^u(O) \backslash O$; then, all points belonging to $\Gamma_1 \cap W^s_{loc}(O)$ and $\Gamma_2 \cap W^s_{loc}(O)$ reside exactly in the same part

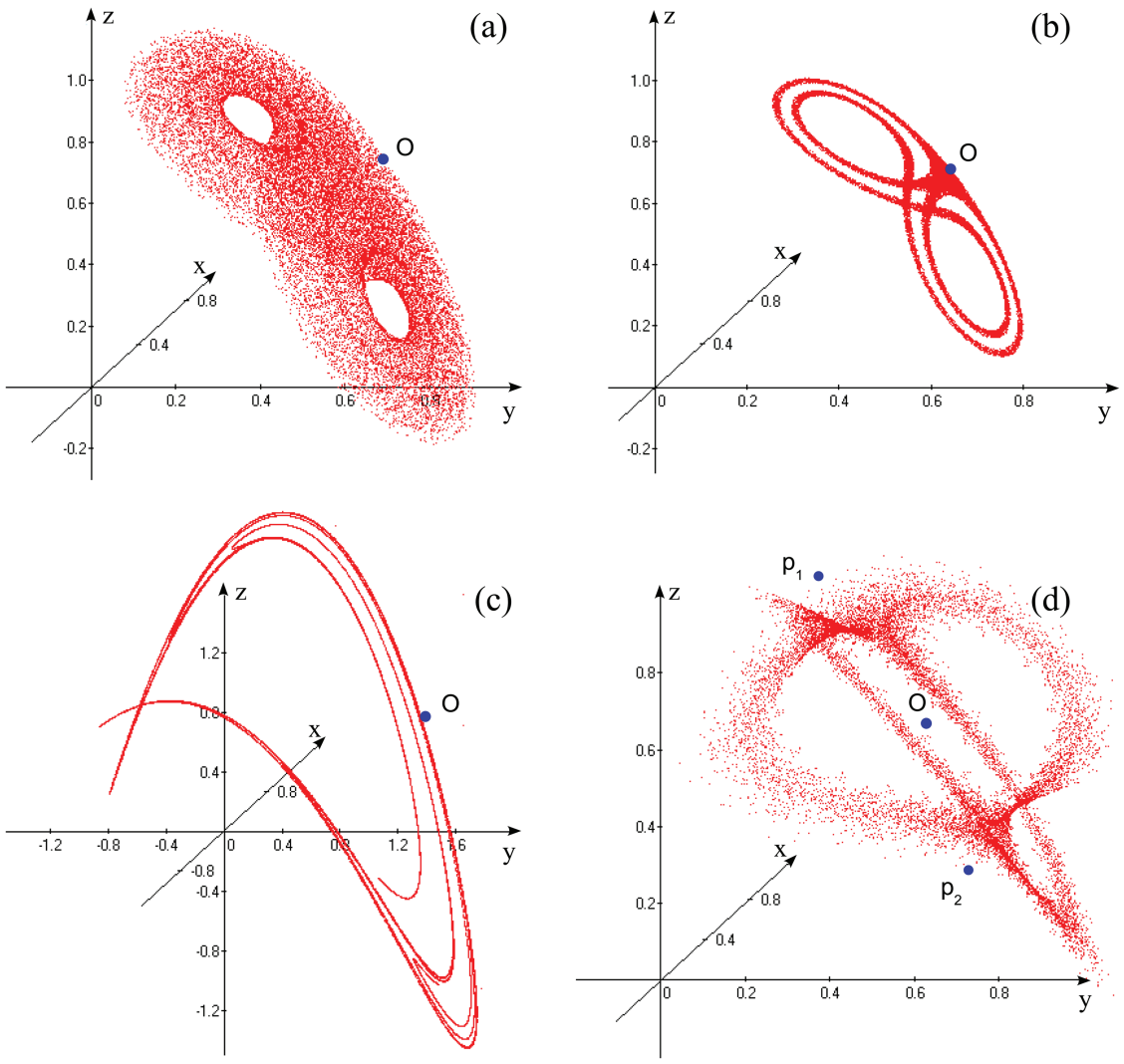

FIG. 1. Plots of attractors of map (1), based on Ref. 3. Figures (a) and (b): discrete Lorenz-like attractors at $B = 0.7; M_1 = 0$; (a) $M_2 = 0.85$; and (b) $M_2 = 0.815$. Figure (c): an attractor similar to the 2D Hénon attractor for $B = 0.1; M_1 = 1.4;$ and $M_2 = 0.2$. Figure (d): a period-2 attractor (containing period-2 saddles p_1 and p_2) for $B = -0.95; M_1 = 1.77;$ and $M_2 = -0.925$. For each plots, there are shown about 10^5 forward iterations of some initial point after a large number of preliminary iterations.

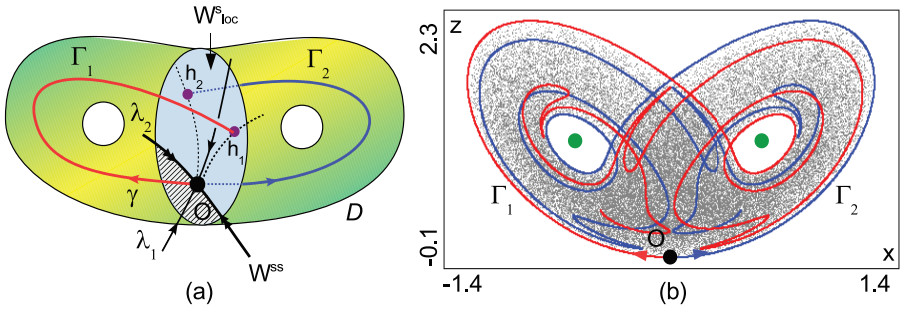

FIG. 2. (a) Skeleton scheme for a discrete Lorenz-like attractor: D is an adsorbing domain (a solid pretzel); the curves $\Gamma_i \cup [h_i, O]$ are non-contractible in D; h_1 and h_2 reside in the same part of $W^s_{loc} \backslash W^{ss}$. (b) Periodically perturbed the Lorenz attractor in the Poincaré map by period $t = 2\pi$ of the Shimizu–Morioka system (5) (here, $\alpha = 0.35, \lambda = 0.9$ with the perturbation $\varepsilon z \sin t$ in $\dot{z}$, where $\varepsilon = 0.01$).

of the set $W^s_{loc}(O) \backslash W^{ss}(O)$ [see Fig. 2(a)] [and also Figs. 3(b) and 4(b)]; and

(iii) there is an adsorbing domain D for A that has a solid pretzel shape (a ball with two holes) and such that a closed curve $\mathcal{L}_i, i = 1, 2$, is non-contractible in D, where $\mathcal{L}_i$ is composed from a piece of Γ_i from O to the point h_i of the first intersection of Γ_i with W^s_{loc} and a simple arc between h_i and O [see Fig. 2(a)].

As an example, we show in Fig. 2(b) an attractor in the Poincaré map for period $t = 2\pi$ in a periodically perturbed Shimizu–Morioka model (5) with the additional term $\varepsilon z \sin t$ in the right side of $\dot{z}$, where $\varepsilon = 0.01$. One can check that conditions (i)–(iii) are fulfilled for this attractor. In particular, here $\gamma = 58.13, \lambda_1 = 0.11$, $\lambda_2 = 6.02 \times 10^{-5}$. By the way, in the case of the attractors in Figs. 1(a) and 1(b), the point O has eigenvalues $\gamma = -1.35$, $\lambda_1 = 0.85, \lambda_2 = -0.6$, and $\gamma = -1.23, \lambda_1 = 0.86, \lambda_2 = -0.66$, respectively.

Discrete attractors in Figs. 1(a), 1(b), and 2(b) are certainly Lorenz-like ones. Moreover, as in the case of flow attractors, we can see a certain difference between these attractors: the attractors in Figs. 1(a) and 2(b) look homogenous, without lacunae, while the attractor in Fig. 1(b) has a lacuna. Recall that in the case of the classical Lorenz attractor, a (trivial) lacuna is an open region (a hole inside the attractor) that contains a saddle limit cycle whose stable manifold does not intersect the attractor.[2] Accordingly, in the case of a discrete Lorenz-like attractor, a lacuna contains a saddle closed invariant curve with the same property. When varying parameters, lacunae can appear and disappear due to the appearance/disappearance of homoclinic intersections. The corresponding bifurcations belong to the class of the so-called internal bifurcations of attractor (see more details in Refs. 2, 22, and 23).

The attractor presented in Fig. 1(c) is also a discrete homoclinic attractor [it contains the fixed point $O(x = y = z \approx 0.88)$], which is similar to the two-dimensional Hénon attractor,[10] while the attractors in Figs. 1(a), 1(b), and 1(d) are essentially three-dimensional. Besides, the attractor in Fig. 1(d) is nonorientable (here, $B = -0.95 < 0$), and it contains a period-2 saddle orbit (p_1, p_2) but does not contain fixed points. In the case under consideration, $p_1 = (x_0, y_0, x_0)$ and $p_2 = (y_0, x_0, y_0)$, where $x_0 \approx 0.85$ and $y_0 \approx 0.126$.

Note that map (1) is a representative of a class of maps

$$\bar{x} = y, \quad \bar{y} = z, \quad \bar{z} = Bx + G(y, z), \tag{2}$$

which are called *three-dimensional generalized Hénon maps*. Such maps have the constant Jacobian B and are, in a sense, the simplest three-dimensional nonlinear maps. Because of this, their use for the purpose of searching and studying strange attractors, including homoclinic ones, is very convenient and beneficial in many respects. Therefore, we use maps of form (2) as a source of main examples illustrating our results (see also Ref. 20).

In Sec. II, we give a qualitative description of the discrete Lorenz-like attractors dealing more accent to their geometric properties and a comparison with the classical Lorenz attractors of three-dimensional flows. We discuss also on geometric properties of other types of discrete Lorenz-like attractors for orientable and nonorientable three-dimensional maps.

One of remarkable properties of discrete homoclinic attractors, including the mentioned above discrete Lorenz-like attractors, consists in the fact that they can arise in various kinds of models as a result of rather simple and universal bifurcation scenarios. Moreover, these scenarios can be freely observed in one-parameter families starting from those parameter values when the attractor is simple, e.g., a stable fixed point.[17,19] In Sec. III, we consider these scenarios phenomenologically and supplement them with new content, focusing on those bifurcations that support geometric structures of discrete Lorenz-type attractors that may arise. Thus, the proposed modified scenarios are not only phenomenological, as presented in Refs. 17 and 19, but also empirical, since they can be confirmed by numerical experiments.

We show two typical examples of implementation of these scenarios in the case of the three-dimensional Hénon map (1) (see Fig. 7), and in the case of Poincaré map for a Celtic stone model (see Fig. 8). For comparison, we also schematically show in Fig. 9 the well-known scenario (see, for example, Ref. 24), of the Lorenz attractor appearance in the one-parameter family of the Lorenz model

$$\dot{x} = -\sigma(x - y), \ \dot{y} = -xz + rx - y, \ \dot{z} = xy - bz, \tag{3}$$

where the parameters b and σ are fixed, $b = 8/3, \sigma = 10$, and the parameter r is governing. Note that if we compare the two scenarios, in the case of a Celtic stone model (see Fig. 8), and in the case of the Lorenz model (see Fig. 9), the first thing that catches your eye is the astonishing similarity in their main details.

The fact that discrete Lorenz-like attractors can appear as a result of very simple and realistic bifurcation scenarios shows that they should be met in various models from applications. As we know, the first such model is a nonholonomic model of Celtic

stone.[25] More recently, discrete Lorenz-like attractors were also found in models of diffusion convection.[26,27]

In Sec. IV, we discuss one more, perhaps the most interesting, fundamental property of discrete Lorenz attractors related to the fact that they can be genuine strange attractors, i.e., robustly preserving their chaoticity at perturbations. Recall that, as is commonly believed, a strange attractor is considered genuine, if *all* its orbits have the positive maximal Lyapunov exponent and this property is open, i.e., holds for all close systems (in the C^r-topology with $r \geq 1$).

Until recently, only hyperbolic attractors and flow Lorenz-like attractors (the latter belong to the class of singular hyperbolic attractors[28,29]) could reliably be considered as genuine strange attractors. However, in the work by Turaev and Shilnikov,[30] one more class of genuine strange attractors, the so-called *pseudohyperbolic attractors*, was introduced and, moreover, a geometric model of such an attractor for flows in dimension four and higher was constructed. This attractor was called in Ref. 30 wild spiral attractor, since it contains a saddle-focus equilibrium together with wild hyperbolic subsets and, hence, it allows homoclinic tangencies, i.e., nontransversal intersections of stable and unstable invariant manifolds of the same saddle periodic orbit. Despite the fact that such attractors were predicted (as well as geometrically constructed) in the late 1990s, the first example of such an attractor in a concrete system of four differential equations was found much recently in Ref. 31.

Remark 1. The wild hyperbolic sets were discovered by Newhouse.[32,33] He used the term "wild" for the notation of uniformly hyperbolic sets whose stable and unstable invariant manifolds have nontransversal intersections and this property holds for all C^r-close systems with $r \geq 2$. Thus, such systems compose open regions (the so-called Newhouse regions) in the space of dynamical systems and systems with homoclinic tangencies are dense in these regions. The existence of Newhouse regions near any multidimensional system with a homoclinic tangency was proven in Refs. 34–36.

Discrete Lorenz-like attractors, in particular, those discovered in Ref. 3, consist one more class of wild pseudohyperbolic attractors in the case of three-dimensional maps. Note also that wild pseudohyperbolic attractors are not uniformly hyperbolic, since they admit homoclinic tangencies and arbitrary degenerate bifurcations[37–39] that, nevertheless, do not lead to periodic sinks and, therefore, do not destroy chaoticity. Discrete Lorenz-like attractors, in contrast to the flow Lorenz attractors, are wild (admit homoclinic tangencies)—this fact is simple and almost evident—in any case, its numerical evidence was demonstrated in Ref. 20.

In Sec. IV, we give a definition of pseudohyperbolic invariant sets of multidimensional diffeomorphisms (Definition 1) and explain how it can be adapted to the discrete Lorenz-like attractors of three-dimensional maps. First, we discuss local aspects of the corresponding theory related to the fact that such attractors can be born under codimension-3 bifurcations of fixed points. This allows us to say about the "existence of genuine discrete Lorenz-like attractors." Second, we apply a quite simple numerical method [the so-called Light Method of Pseudohyperbolicity (LMP) method[31,40]] to test the pseudohyperbolicity of attractors when the above local theory is not applicable. The results for the attractors presented in Figs. 1(a) and 1(b) are illustrated in Figs. 10(a) and 10(b) in the form of corresponding LMP-graphs. Thus, in Sec. IV, we demonstrate a numerical evidence for pseudohyperbolicity of attractors under consideration.

Main results of Sec. V are essentially new. In particular, we provide one more type of bifurcation scenarios leading to the appearance of the so-called period-2 Lorenz-like attractors and give an example of the implementation of such a scenario in the case of the nonorientable maps of the form (1) with $B = -0.8$ (see Fig. 12). We study the dynamical and geometrical properties of period-2 Lorenz-like attractors and show that these attractors can undergo crises leading to the emergence of strange homoclinic and heteroclinic attractors of new types. We construct geometric (skeleton) schemes of these attractors and their phase portraits in map (1) (see Figs. 13–15). We show also that the period-2 Lorenz-like attractor, as well as emerging after its crisis the period-2 heteroclinic attractor, can be genuinely pseudohyperbolic. On the other hand, the found homoclinic attractors, containing the fixed point O and a period-2 orbit [see some example in Fig. 14(b)], are not pseudohyperbolic because the point O is a saddle-focus. Moreover, this point has a pair of complex conjugate eigenvalues (multipliers) close to the 1:4 resonance (i.e., $\lambda_{1,2} = \rho\, e^{\pm i\varphi}$, where φ is close to $\pi/2$ and $\rho < 1$ is close to 1). Thus, we also, indirectly, have touched the problem,[17] on the structure of emerging homoclinic attractors when passing near strong resonances.

In Sec. VI, we discuss a series of open problems associated with the study of discrete homoclinic attractors, emphasizing especial attention to those ones that are related to discrete Lorenz-like attractors.

II. ON GEOMETRICAL PROPERTIES OF DISCRETE LORENZ-LIKE ATTRACTORS OF THREE-DIMENSIONAL DIFFEOMORPHISMS

By definition, the discrete homoclinic attractors of maps are strange attractors containing a single saddle fixed point. Therefore, one of the main characteristics of such an attractor is the topological type of its fixed point that is defined as follows.

Let O be a fixed point of a three-dimensional diffeomorphism T and $\lambda_1, \lambda_2, \lambda_3$ be the multipliers of O, i.e., eigenvalues of the linearization matrix for T calculated at O. Let also O be the hyperbolic point, i.e., $|\lambda_i| \neq 1$. Then, we say that the point O is of type (m, n), if it has m stable and n unstable multipliers, which, respectively, are less than 1 and greater than 1 in the absolute value. The type of a hyperbolic q-periodic orbit is determined similarly by the multipliers of the map T^q at any of its points.

Thus, in the three-dimensional case, hyperbolic fixed (periodic) points may be of four types: (3,0)—stable (sinks), (0,3)—completely unstable (sources), and saddle fixed points of types (2,1) and (1,2). Besides, saddle fixed points are divided into *saddles*, when all their three multipliers are real, and *saddle-foci*, when a pair of complex conjugate multipliers exists.

In the last case, the corresponding discrete homoclinic attractors are usually called spiral. These attractors, according to Refs. 17 and 20, are divided into two groups of attractors: discrete figure-8 spiral attractors, when they contain a saddle-focus of type (2,1), and discrete Shilnikov attractors, when they contain a saddle-focus of type (1,2). Such discrete spiral attractors are often met in various applications (see, e.g., Refs. 41–45). As for the discrete Shilnikov

attractors, they are also interesting from the point of view that they can give simple criteria for hyperchaos in four-dimensional flows and three-dimensional maps.[44,45]

When the point O is a saddle, the classification of the corresponding homoclinic attractors is more variable. So, homoclinic attractors with a saddle fixed point of type (2,1) may be, except for Lorenz-like one, of such types as figure-8, double figure-8, double Lorenz-like, etc. (see, e.g., Refs. 20 and 46). Discrete homoclinic attractors with saddles of type (1,2) also differ in variety, but they are still poorly understood (for some examples, see Ref. 20).

As we said before, discrete Lorenz-like attractors were first found in Ref. 3, see the corresponding examples in Figs. 1(a) and 1(b). Attractors in these figures contain a saddle fixed point O of type (2,1) with multipliers $\lambda_1, \lambda_2, \gamma$ satisfying the following conditions:

$$\begin{aligned} &\text{(a) } 0 < \lambda_1 < 1,\ -1 < \lambda_2 < 0,\ \gamma < -1,\ |\lambda_1\lambda_2\gamma| < 1,\\ &\text{(b) } |\lambda_1| > |\lambda_2|, \qquad (4)\\ &\text{(c) } \sigma = |\lambda_1\gamma| > 1. \end{aligned}$$

The quantity σ is called the saddle value and it is defined, for a hyperbolic saddle periodic orbit, as the absolute value of product of two nearest to the unit circle stable and unstable multipliers.

It is interesting that, using only conditions (4) and certain geometrical considerations, one can easily imagine what kind of a homoclinic attractor with the point O can arise here (see Fig. 3). Below, we will try to argue for this.

By virtue of (4), the unstable invariant manifold $W^u(O)$ of the point O is one-dimensional and, hence, it is divided by the point O into two connected components—separatrices W^{u+} and W^{u-}. Since the unstable multiplier γ of O is negative, $\gamma < -1$, the separatrices W^{u+} and W^{u-} are invariant under T^2 and such that $T(W^{u+}) = W^{u-}$ and $T(W^{u-}) = W^{u+}$. That is, under iterations of T, points of W^u jump alternately from one separatrix to another. The stable invariant manifold $W^s(O)$ of the point O is two-dimensional, and the map $T_s = T|_{W^s_{loc}}$ [i.e., the restriction of T into the local stable manifold $W^s_{loc}(O)$] has a fixed point $\tilde{O} = O \cap W^s_{loc}$ that is a nonorientable node. By virtue of (4)(a) and (4)(b), in W^s_{loc}, there is the so-called strong stable invariant manifold W^{ss} that is a curve touching at $\tilde{O}$ to the eigendirection corresponding to the strong stable multiplier $\lambda_2 < 0$. Note that the curve W^{ss} divides W^s_{loc} into two parts, Π_1 and Π_2, and, since $\lambda_1 > 0$, points from Π_1 cannot jump to Π_2 (and otherwise) under iterations of T_s [see Fig. 3(a)].

The two-dimensional map T_s can be viewed, for simplicity, as a linear map of the form $\bar{x} = \lambda_1 x, \bar{y} = \lambda_2 y$, where $-1 < \lambda_2 < 0 < \lambda_1 < 1$ and $|\lambda_2| < |\lambda_1|$. Then, W^{ss} has the equation $x = 0$, and $\Pi_1 = \{(x,y)|x > 0\}$, $\Pi_2 = \{(x,y)|x < 0\}$. Moreover, as it is well known, a neighborhood of the point $\tilde{O}$ is foliated into invariant (under T_s^2) curves $\{l_c\}$ of form $y = c|x|^\alpha$, where $\alpha = \ln|\lambda_2|/\ln|\lambda_1|$. All these curves, except for the curve $x = 0$, enter $\tilde{O}$ touching the axis $y = 0$. Let a point $h_1(x_1, y_1)$ belong to some curve $y = cx^\alpha$ with $x > 0$ [or $y = c(-x)^\alpha$ with $x < 0$]. Then, its image, the point $h_2 = T_s(h_1) = (\lambda_1 x_1, \lambda_2 y_1)$, will belong to the curve $y = -cx^\alpha$ [respectively, $y = -c(-x)^\alpha$]. If $c \neq 0$, these two curves compose the boundary of an exponentially narrow wedge adjacent to the point $\tilde{O}$ on one side [e.g., on Π_1 as in Fig. 3(a)—here the wedge is given by the inequalities $|y| \le c_1 x^\alpha, x \ge 0$, where the constant c_1 is defined by the initial data (x_1, y_1), namely, $c_1 = y_1 x_1^{-\alpha}$]. Evidently, forward iterations under T_s of the point h_1, i.e., the points $h_1, h_2, \ldots$, where $h_{i+1} = T_s(h_i)$, jump alternately on the sides of this wedge and accumulate to the point O as $i \to +\infty$.

Now, one can imagine that h_1 is an intersection point of W^{u+} with W^s. Then, h_2 is the intersection point of W^{u-} with W^s, since $T(W^{u+}) = W^{u-}$, and h_3 is again the intersection point of W^{u+} with W^s, etc. Correspondingly, the points $h_1, h_2, \ldots$, are points of some

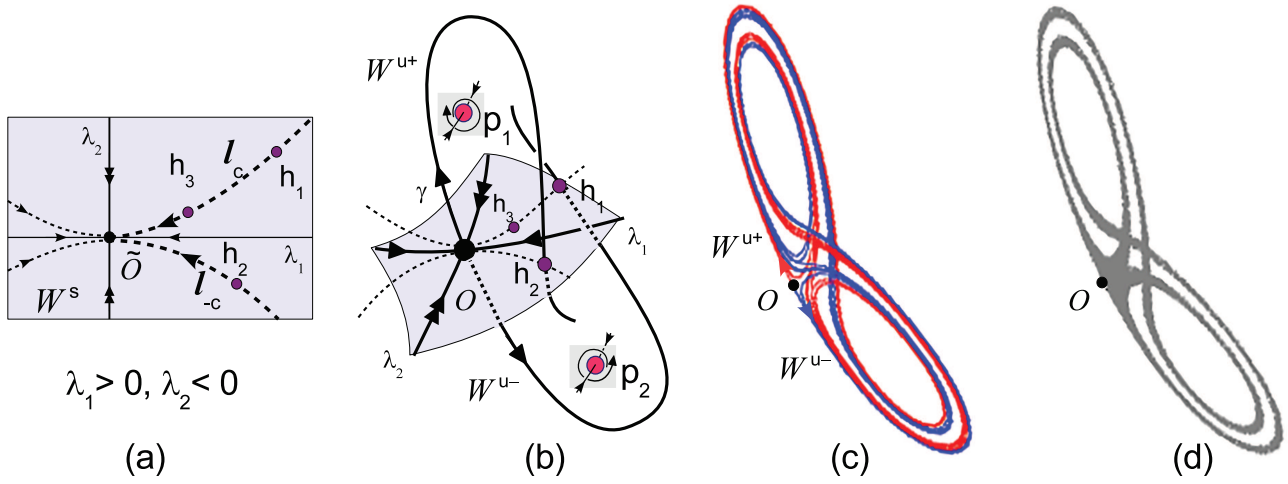

FIG. 3. (a) An illustration for orbits behavior near a nonorientable sink $\tilde{O}$ having multipliers $-1 < \lambda_2 < 0 < \lambda_1 < 1$, where $|\lambda_2| < |\lambda_1|$; (b) a schematic homoclinic butterfly configuration of semi-global pieces of one-dimensional unstable invariant manifolds of the saddle point O of type (2,1). In Figs. (c) and (d), phase portraits for the case of map (1) with $B = 0.7$; $M_1 = 0$; and $M_2 = 0.815$ are shown: (c) a picture of the separatrices W^{u+} and W^{u-} of the saddle O; and (d) a plot of the homoclinic attractor in an appropriate two-dimensional projection.

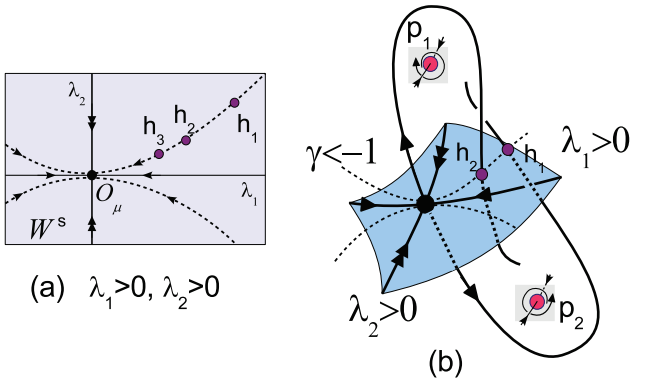

FIG. 4. (a) Behavior of iterations of points near a stable node with $0 < \lambda_2 < \lambda_1 < 1$. (b) A homoclinic-butterfly configuration of semi-global pieces of unstable separatrices of a nonorientable saddle with multipliers $0 < \lambda_2 < \lambda_1 < 1$ and $\gamma < -1$.

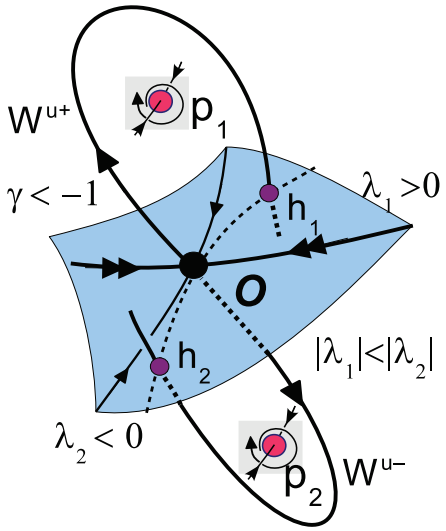

FIG. 5. A homoclinic figure-8 configuration of W^{u+} and W^{u-}.

homoclinic to O orbit, i.e., an orbit entirely lying in the invariant set $W^u(O) \cap W^s(O)$ and distinct of O. We call the points $h_1, h_2, \ldots$, *primary homoclinic points*. Evidently, their disposition in W^s_{loc} defines in much a skeleton of a homoclinic attractor that, in turn, can be viewed as the closure of the unstable manifold $W^u(O)$.

It is easy to see that the configuration of semi-global pieces of W^{u+} and W^{u-}, until the first their intersections with W^s_{loc} [see Fig. 3(b)], is similar to the configuration of homoclinic butterfly in the Lorenz model (3) [compare with Fig. 9(b)]. In order to fill this construction with more geometric content, we additionally show in Fig. 3(b) two points p_1 and p_2, which, by analogy with the classical Lorenz attractor, must be saddle points of type (1,2), whereas the point O is of type (2,1). Since the unstable multiplier γ is negative, it evidently follows that p_1 and p_2 are points of the same saddle period-2 orbit [i.e., $T(p_1) = p_2$ and $T(p_2) = p_1$]. Besides, the points p_1 and p_2 should reside in two "holes" of the attractor, which only emphasizes its similarity with the Lorenz attractor.

Note that analogous geometric considerations can be applied also for three-dimensional nonorientable maps. For example, let such a map T have a fixed point O with multipliers λ_1, λ_2 and γ such that $0 < \lambda_2 < \lambda_1 < 1, \gamma < -1$ (and $-1 < \lambda_1\lambda_2\gamma < 0$). As in the previous case, the point O is a saddle of type (2,1); however, the corresponding map $T_s = T|_{W^s_{loc}}$ has a fixed point $\tilde{O} = O \cap W^s_{loc}$ that is an orientable node [Fig. 4(a)]. Therefore, if T has a homoclinic to O orbit, then its points $h_1, h_2, \ldots$, on W^s_{loc} will belong to the same invariant curve of the form $y = C|x|^\alpha$ [see Fig. 4(b)], in distinct of the case of orientable attractor [Fig. 3(a)], where such homoclinic points lie alternately on boundaries of an exponentially narrow wedge. We see that the difference looks to be very insignificant, and, in principle, it does not prevent a possible attractor from having a Lorenz-like structure. However, we need to say that any genuine discrete homoclinic Lorenz-like attractors (with a fixed point) were not found yet in maps of the form (2) with $B < 0$ (everything that is more or less similar turned out to be quasiattractors). On the other hand, much more interesting results on this topic are presented in Section V, which are related to the existence of genuine period-2 Lorenz-like attractors in three-dimensional nonorientable maps.

Remark 2. Conditions of (4) are very important. In particular, if condition (4)(b) is violated, i.e., $|\lambda_2| > |\lambda_1|$, then a possible homoclinic attractor is the so-called discrete figure-8 attractor.[17,20,47] For this case, a schematic configuration of semi-global pieces of the one-dimensional unstable invariant manifold of the point O is shown in Fig. 5 [compare it with Fig. 3(b)].

III. ON PHENOMENOLOGICAL SCENARIOS OF THE ONSET OF DISCRETE LORENZ-LIKE ATTRACTORS

One of the most interesting peculiarities of discrete homoclinic attractors is that they can occur in one-parameter families of (three-dimensional) maps as a result of quite simple universal bifurcation scenarios.[17,19,20]

The idea of constructing such scenarios goes back to the paper by Shilnikov,[48] in which he described a phenomenological scenario of the spiral chaos appearance in the case of multidimensional flows when a homoclinic attractor emerges containing a saddle-focus equilibrium with the two-dimensional unstable manifold. In Ref. 48, it was also outlined the case when a discrete spiral attractor appears in the Poincaré map of a flow: such an attractor contains only one fixed point that is a saddle-focus with two-dimensional unstable manifold (see Refs. 17 and 19 for more details).

This fully applies to discrete Lorenz-like attractors. Schematically, main stages of the corresponding scenario are shown in Fig. 6 for the case of a one-parameter family T_μ of three-dimensional orientable maps.

This scenario begins from those values of μ where the map T_μ has an asymptotically stable fixed point (sink) O_μ [see Fig. 6(a)]. We assume that, at a certain value of μ, the point O_μ loses its stability under the *supercritical period-doubling bifurcation*: O_μ becomes a saddle of type (2,1) and a stable period-2 orbit (p_1, p_2) is born

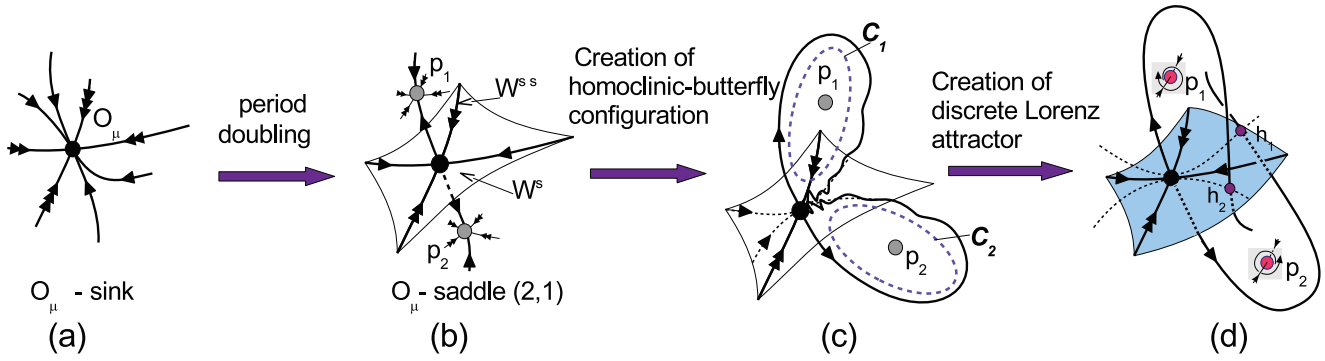

FIG. 6. A phenomenological description of main steps for the scenario of onset of a discrete Lorenz-like attractor: (a) a stable fixed point O_μ; (b) after a period-doubling bifurcation: the point O_μ becomes a saddle of type (2,1) and the attractor now is a period-2 orbit (p_1, p_2); (c) a creation of a homoclinic butterfly configuration for $W^u(O_\mu)$ and a formation of a closed invariant curve (C_1, C_2) of period 2, i.e., $T_\mu(C_1) = C_2$ and $T_\mu(C_2) = C_1$ (this curve is saddle if $\sigma > 1$); and (d) the orbit (p_1, p_2) and all attracting invariant sets generated from it lose stability and a discrete Lorenz-like attractor appears (which can be genuine, and then it will be the only attracting invariant set; see Sec. IV).

which now becomes the attractor [Fig. 6(b)]. Since O_μ undergoes the period-doubling bifurcation, one of its multipliers, λ_1, becomes less than -1, and other two multipliers, λ_2 and λ_3, are real and have different signs, $-1 < \lambda_2 < 0 < \lambda_3 < 1$, due to the orientability of the map. In what follows, we assume that the conditions (4) hold. Then, when the parameter changes, the orbit (p_1, p_2) and all attracting invariant sets generated from it should lose stability as a result of some bifurcations. How this happens depends on specific of the problem. We indicate two the simplest and natural options:

- **[sc1]** the orbit (p_1, p_2) loses the stability under the *subcritical* Andronov–Hopf bifurcation: a period-2 closed invariant curve (C_1, C_2) of saddle type merges with the stable orbit (p_1, p_2) and the latter becomes saddle orbit of type (1,2);
- **[sc2]** the stable orbit (p_1, p_2) undergoes the *supercritical* Andronov–Hopf bifurcation, after which the orbit becomes saddle of type (1,2) and a period-2 stable closed invariant curve (S_1, S_2) is born, and then the stable curve (S_1, S_2) merges with the saddle curve (C_1, C_2) and both disappear.

Note that the above period-2 invariant curve (C_1, C_2) is formed from the homoclinic butterfly configuration of unstable separatrices W^{u+} and W^{u-} of O_μ at that moment when the invariant manifolds of O_μ begin to intersect [see Figs. 6(c), 7(d), and 8(b)]. Besides, the period-2 curve (C_1, C_2) is saddle when $\sigma > 1$ and stable when $\sigma < 1$. We also note that the period-2 curves (C_1, C_2) and (S_1, S_2) from **[sc2]** can merge and disappear, e.g., as result of the Chenciner bifurcation scenarios.[49]

It is worth noting that both cases, **[sc1]** and **[sc2]**, are often met in applications. In particular, examples of their implementation were found in the three-dimensional generalized Hénon maps of form (2) (see, e.g., Refs. 17, 18, and 20) when the value $0 < B < 1$ of the Jacobian is not too small and in a model of Celtic stone.[25,50] Two illustrations of the corresponding scenarios are shown in Figs. 7 and 8.

In Fig. 7, main stages of the scenario of the discrete Lorenz-like attractor formation are shown for the case of a one-parameter family of maps of the form (1) where $B = 0.7, M_2 = 0.85$, and M_1 is the control parameter. The scenario starts from $M_1 \approx -0.076$, when a stable fixed point O is born under a saddle-node bifurcation. At $M_1 \approx -0.053$, the point O undergoes a period-doubling bifurcation after which it becomes a saddle of type (2,1) and a period-2 stable orbit (p_1, p_2) is born. Just after this bifurcation, the orbit (p_1, p_2) is the attractor [Fig. 7(a)]. At $M_1 \approx -0.035\,56$, the orbit (p_1, p_2) undergoes the supercritical Andronov–Hopf bifurcation after which it becomes a period-2 saddle-focus of type (1,2) and a stable period-2 invariant curve (S_1, S_2) is born that is the attractor now [Fig. 7(b)].

However, very quickly, one more attractor appears, the so-called "thin Lorenz attractor," due to the creation of a homoclinic butterfly (that exists for a very thin region of parameters) with the saddle fixed point O [Figs. 7(c) and 7(d)]. At the same time, a period-2 saddle invariant curve (C_1, C_2) emerges from this homoclinic butterfly.

As we know, bifurcations of the formation of closed invariant curves from a discrete homoclinic butterfly (homoclinic figure-8) have not been studied yet in detail. Only certain results are known when there are considered small periodic perturbations of a flow with a homoclinic loop (see, e.g., Ref. 51, where the birth of an invariant circle has been deduced from the annulus principle). Thus, the period-2 curves (C_1, C_2) shown in Figs. 7 and 8 can be considered as only numerically found ones. Moreover, we have here a happy case when these curves can be prolonged in a parameter sufficiently far (usually, they are quickly destroyed). So, in the case of Fig. 7, the curves (S_1, S_2) and (C_1, C_2) merge and both disappear [Figs. 7(d) and 7(e)]. After this, the discrete Lorenz-like attractor becomes the unique attracting set. A behavior of one unstable separatrix of O is shown in Fig. 7(e) (other separatrix behaves symmetrically because the unstable multiplier of O is negative) and the phase portrait of an attractor is shown in Fig. 7(f) (here, O has coordinates $x = y = z \approx 0.51$). Thus, we see that the option **[sc2]** is involved within the scenario.

Remark 3. Note that for the implementation of such a scenario as in Fig. 7, the Jacobian B of map (2) should not be too

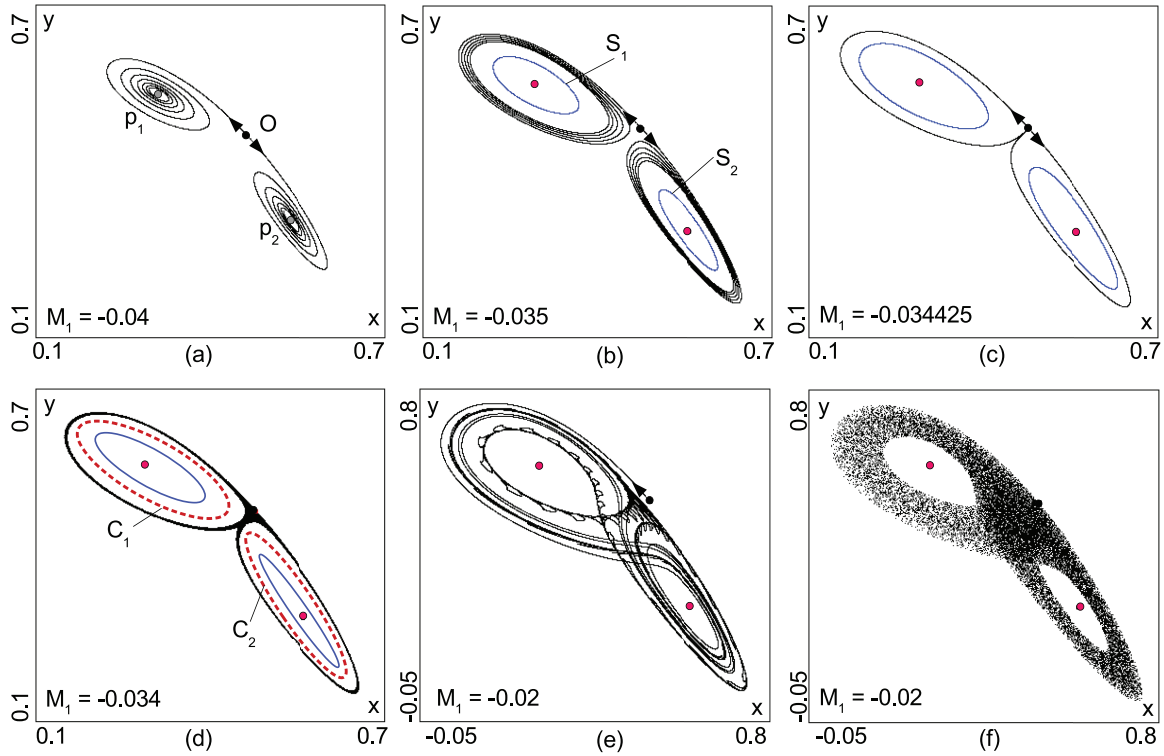

FIG. 7. Evolution of attractors in map (1) with $B = 0.7, M_2 = 0.85$ when varying M_1. Here, the option **[sc2]** of the scenario is realized. In Figs. (a)–(e), behavior of the unstable separatrices of the point O is also shown. In Fig. (f), a phase portrait of the attractor is presented.

small. Otherwise, even if the conditions of (4) hold, the orbit (p_1, p_2) has a tendency to lose its stability via a cascade (finite or infinite) of period-doubling bifurcations [for map (1), this happened when $|B| < \frac{1}{3}$,[3]]. Then, the resulting attractor may not at all resemble the Lorenz attractor: it can be imagined either as a "strongly deformed Lorenz-like attractor" or as a "thickened Hénon-like attractor." That is, a certain analogy between phase portraits of discrete and flow Lorenz attractors cannot be clearly observed and even fully disappear.

A similar picture is observed for the Celtic stone model[50] (see Fig. 8). Only here the option **[sc1]** is realized: the period-2 orbit (p_1, p_2) loses its stability under the subcritical Andronov–Hopf bifurcation when the period-2 saddle invariant curve (C_1, C_2) merges with the stable period-2 orbit (p_1, p_2) and the latter becomes a saddle-focus of type (1,2) and only one attractor remains in the model; this is a discrete Lorenz-like attractor [Fig. 8(f)]. In addition, here one can trace how the unstable separatrices of saddle O are rearranged when passing near values of the parameter E corresponding to the formation of a homoclinic-butterfly with the point O [see Figs. 8(a)–8(c)]. In the case of map (1), this rearrangement, even if it exists, is extremely difficult to catch.

We have proposed scenarios with the options **[sc1]** and **[sc2]**, mainly for two reasons. First is because they obviously support a similarity of the geometry of the resulting discrete homoclinic attractor and the classical Lorenz attractor. Secondly is because the discrete scenarios themselves repeat the flow ones in many principal details. So, in Fig. 9, a schematic picture is shown for the scenario of onset of the Lorenz attractor in the Lorenz model (3) when varying the parameter r. Here, two saddle limit cycles symmetrical to each other are born from a homoclinic butterfly and then these cycles merge with the non-zero stable equilibria, and, just after this subcritical Andronov–Hopf bifurcation, the Lorenz attractor appears to be the unique attracting invariant set of the model. Thus, the flow analog of the option **[sc1]** is realized here.

The same scenario can be also observed in the Shimizu–Morioka model

$$\dot{X} = Y,\ \dot{Y} = X(1 - Z) - \lambda Y,\ \dot{Z} = -\alpha Z - X^2. \qquad (5)$$

However, the flow analog of the option **[sc2]** can also be observed here:[52,53] the non-zero equilibria lose their stability under the supercritical Andronov–Hopf bifurcation and, as result, two stable symmetric each other limit cycles are born and, further, these cycles merge with saddle ones and both disappear.

In general, the stage of the discrete scenarios when a global bifurcation occurs associated with the formation of homoclinic structures at the point O_μ, is a key one. It indicates the appearance

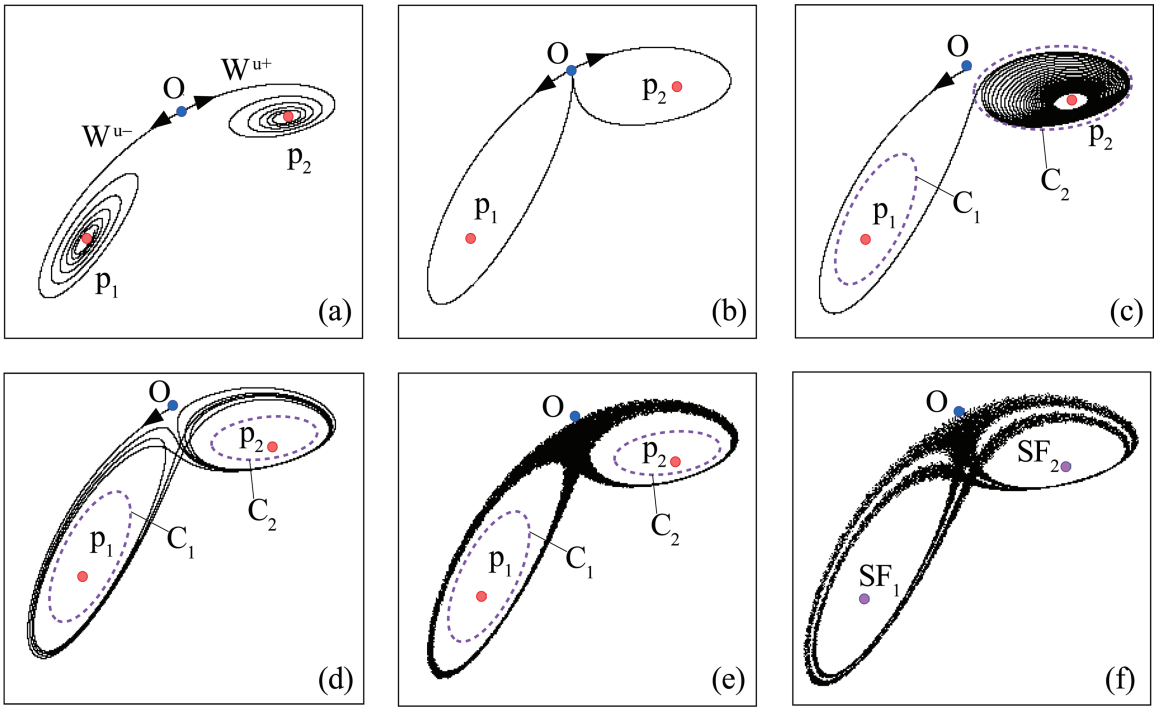

FIG. 8. Evolution of attractors in a nonholonomic model of Celtic stone, based on Ref. 50, when varying a parameter E (the full energy of the stone): (a)–(e) the period-2 orbit $P = (p_1, p_2)$ is attractor; (b) a "thin Lorenz attractor" can also exist for an extremely small interval of values of E; (d)–(e) the discrete Lorenz-like attractor LA coexists with the stable orbit P; (e) a behavior of the unstable separatrix of the point O is shown [compare with (c)]; and (f) LA is the only attractor of the model. Here, the option **[sc1]** of the scenario is realized.

of complicated dynamics of the map, and, if the unstable invariant manifold $W^u(O_\mu)$ entirely lies in the absorbing region, then a discrete homoclinic attractor can emerge. Initially, this attractor can coexist with other stable regimes, e.g., with the stable period-2 orbit (p_1, p_2) [see Figs. 7(d) and 8(d)]. However, when the latter has lost the stability, the homoclinic attractor can remain the unique attracting set of the map (see Sec. IV).

As we have explained above, when conditions (4) hold, the corresponding discrete homoclinic attractor can take a shape of the Lorenz attractor. However, we are dealing here with its discrete version, when the fixed point O_μ plays a role of the zero equilibrium of the Lorenz system (3) and the saddle orbit (p_1, p_2) of period 2 resides inside the "holes," instead of two non-zero equilibria O_1 and O_2. In addition, the one-dimensional unstable manifold $W^u(O_\mu)$ consists of two connected components, separatrices W^{u+} and W^{u-}, and, since the unstable multiplier γ of O_μ is negative, $\gamma < -1$, the points on $W^u(O_\mu)$ will "jump" from one separatrix to another, whereas in the classical Lorenz attractor, each of the separatrices of zero equilibrium is invariant itself. Note also that conditions (4)(a) and (4)(b) mean that the unstable and strong stable multipliers of the fixed point O are negative. This provides, in turn, a semi-local symmetry (on invariant manifolds of O) within the discrete attractor, and, in fact, this symmetry plays the same role as the global symmetry $x \to -x, y \to -y, z \to z$ for the Lorenz model (3).

IV. PSEUDOHYPERBOLICITY OF DISCRETE LORENZ-LIKE ATTRACTORS

It is worth noting that the discrete Lorenz attractor, like its flow analog, can be the genuine and only attractor in the corresponding absorbing domain. We say at once that the condition $\sigma > 1$ is simply necessary for this fact. First, when $\sigma < 1$, a homoclinic attractor may not appear at all. In this case, under a homoclinic-butterfly bifurcation, stable invariant curves can be formed, which themselves are attractors and their further evolution can lead to various strange attractors (for example, of torus-chaos type[54]) that are not homoclinic at all. Second, even if a discrete Lorenz shape attractor arises, it will always be the quasiattractor in the case $\sigma < 1$. That is, it is an attractor that looks strange, but only from the "physical point of view,"[55] since it either itself contains stable periodic orbits with very narrow domains of attraction, or such orbits appear under arbitrary small perturbations. Usually, such stable orbits are not detected in experiments and the attractor seems chaotic, but, sometimes, these orbits come to light for certain values of parameters called windows of stability.

One of the main reasons for such nonrobust chaoticity of homoclinic quasiattractors is the inevitable appearance of homoclinic tangencies, i.e., nontransversal intersections of stable and unstable invariant manifolds of the saddle fixed point. When $\sigma < 1$, bifurcations of such tangencies lead to the birth of stable periodic

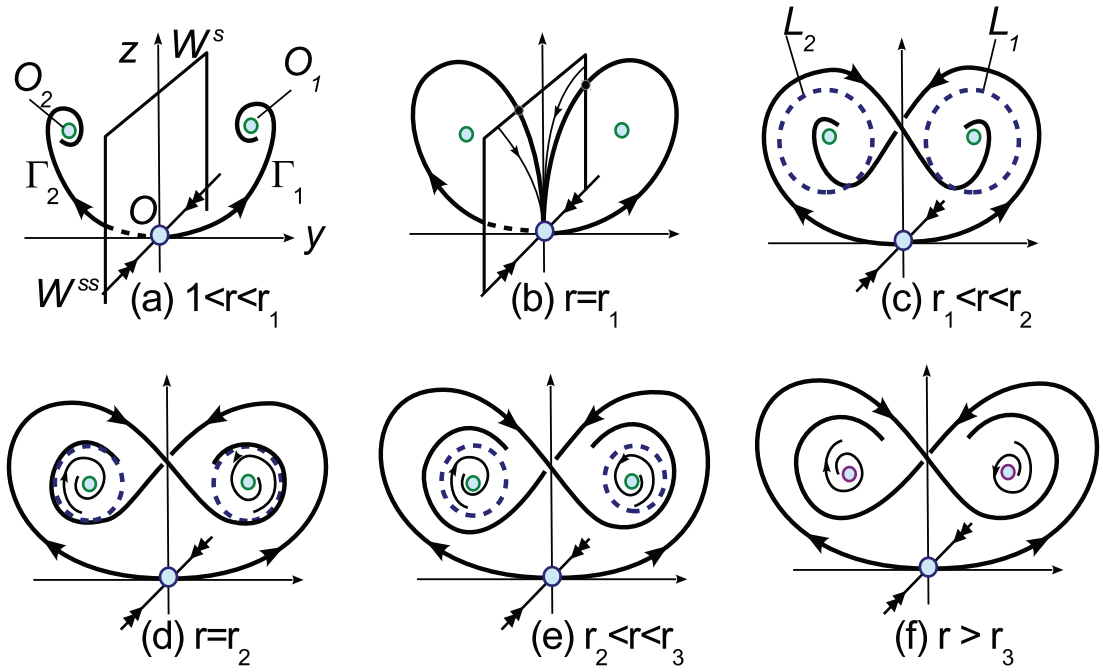

FIG. 9. A sketch of the scenario of onset of the Lorenz attractor in the Lorenz model (3) with $b = 8/3$, $\sigma = 10$ and varying r, based on Ref. 24. Here, $r_1 \approx 13.92$, $r_2 \approx 24.06$, and $r_3 \approx 25.06$. (a) The attractors are non-zero equilibria O_1 and O_2; (b) the homoclinic-butterfly is created; (c) saddle limit cycles L_1 and L_2 are born; (d) the separatrices Γ_1 and Γ_2 belong to the stable manifolds of the limit cycles L_2 and L_1, respectively; (e) multistability: the Lorenz attractor coexists with the attractors O_1 and O_2; and (f) O_1 and O_2 simultaneously lose stability under the subcritical Andronov–Hopf bifurcation and the Lorenz attractor becomes the unique attractor of the model.

orbits.[56–58] The latter have, as a rule, very narrow domains of attraction and big periods. However, everything can change in the case $\sigma > 1$. Here, in general, homoclinic tangencies do not destroy the chaoticity (their bifurcations lead to the birth of saddle periodic orbits,[39,59] instead stable ones). Therefore, the discrete Lorenz-like attractors can keep their chaoticity when changing parameters. Such robustness of chaos is a direct consequence of the fact that the discrete Lorenz-like attractors can be pseudohyperbolic.

Speaking shortly, an attractor is *pseudohyperbolic* if a certain weakened version of hyperbolicity is fulfilled for all its orbits. The concept of pseudohyperbolicity was introduced by Turaev and Shilnikov.[30] For an n-dimensional diffeomorphism T that possesses a closed invariant set $\mathcal{A}$ (e.g., attractor), this can be formulated as follows (for more details, see Refs. 31 and 40).

Definition 1. The set $\mathcal{A}$ is `pseudohyperbolic`, if at every point $x \in \mathcal{A}$, two transversal linear subspaces $N_1(x)$ and $N_2(x)$ exist such that

(i) $\dim N_1 = k, \dim N_2 = n - k$, where $1 \le k \le n - 1$;
(ii) $N_1(x)$ and $N_2(x)$ depend continuously on x;
(iii) $N_1(x)$ and $N_2(x)$ are invariant with respect to the differential DT of the map T, i.e., $DT(N_1(x)) = N_1(f(x))$, $DT(N_2(x)) = N_2(f(x))$;
(iv) DT is exponentially contracting in N_1, and DT expands exponentially all $(n-k)$-dimensional volumes in N_2—this means that there exist such constants $C > 0, 0 < \delta < 1, \nu > 1$ that $\|DT^n(N_1(x))\| < C\delta^n$ and $\left|\det\left(DT^n(N_2(x))\right)\right| > C\nu^n$ for all $n > 0$; and
(v) any possible contraction in N_2 is uniformly weaker than any contraction in N_1.

Note that if condition (iv) from this definition is changed to the much stronger condition

- (iv$_{hyp}$) DT is exponentially contracting in N_1 and DT stretches exponentially all vectors in N_2,

i.e., $\|DT^n(N_1(x))\| < C\delta^n$ and $\|DT^{-n}(N_2(x))\| < C\nu^{-n}$ for all $n > 0$, then we obtain a definition for hyperbolic attractor. However, this hyperbolic condition (iv$_{hyp}$) looks to be very restrictive and, in any case, it does not hold for homoclinic attractors. Nevertheless, discrete hyperbolic attractors are found in applications. It is worth noting that the applied theory of hyperbolicity was essentially developed by Kuznetsov, and, in particular, many relevant examples of physical systems with such attractors were given in his book.[60]

On the other hand, nontrivial examples of pseudohyperbolic homoclinic attractors exist (see, e.g., Refs. 8, 16, 30, 31,and 40). However, in a general setting, the problem of searching for genuine (pseudohyperbolic) attractors seems to be wide open, because it is mainly related to the fundamental problem of distinguishing between genuine attractors and quasiattractors. Only for some types of strange attractors, their pseudohyperbolicity has been proved. In particular, this relates to the discrete Lorenz-like attractors (see, e.g.,

Refs. 3and 16). The results obtained in this direction seem to be very important since the existence of discrete Lorenz-like attractors in three-dimensional maps should be quite common. This, in particular, is due to the fact that such attractors can arise as a result of rather simple global scenarios described in Sec. III, as well as a result of local bifurcations, which we discuss below.

A. Discrete Lorenz-like attractors under local bifurcations

In Ref. 7, it was shown that the flow Lorenz attractors can be born as a result of local bifurcations of an equilibrium with three zero eigenvalues. In the same paper, it was also noted that, in the case of three-dimensional maps, local bifurcations of a fixed point with a triplet $(-1,-1,+1)$ of multipliers can lead to the birth of discrete Lorenz-like attractors. In this case, as was shown in Ref. 3, the second power of the map may be locally (near the fixed point) represented as a map $o(\tau)$-close to the time-τ map of the Shimizu–Morioka system (5), where τ can be taken as small as we want. Since system (5) has the Lorenz attractor for some open domain of positive parameters (α,λ) (see Refs. 9, 52, and 53), it follows that the original map has an attractor that, if to take every second iteration, is a τ-periodic perturbation of the Lorenz attractor.

Map (1) turned out to be the first concrete model in which such codimension-3 bifurcation was studied.[3] Note that map (1) has the fixed point with the triplet $(-1,-1,+1)$ of multipliers for the values $A^*=(M_1=-1/4, M_2=1, B=1)$ of the parameters. It was shown in Ref. 3 that a small discrete Lorenz-like attractor exists in (1) for some domain of the parameters adjoining A^* from the half-space $B<1$.

In Ref. 18, this result was extended to the case of three-dimensional generalized Hénon maps (2). When map (2) has a fixed point, this point can be moved to the origin, and then the map takes the form

$$\bar{x}=y,\ \bar{y}=z,\ \bar{z}=Bx+Cy+Az+ay^2+byz+cy^2+\cdots, \quad (6)$$

where the dots stand for cubic and higher order terms. The characteristic equation at the fixed point $O(0,0,0)$ has the form $\lambda^3-A\lambda^2-C\lambda-B=0$. Thus, the point O has multipliers $(+1,-1,-1)$ at $(A=-1,\ C=1,\ B=1)$ and, hence, for nearby values of the parameters, $B=1-\varepsilon_1, C=1-\varepsilon_2, A=1-\varepsilon_3$, map (6) can be written as

$$\bar{x}=y,\ \bar{y}=z,\ \bar{z}=(1-\varepsilon_1)x+(1-\varepsilon_2)y-(1+\varepsilon_3)z + ay^2+byz+cy^2+\cdots. \quad (7)$$

The following result was established in Ref. 18 (see Lemma 3.1 there).

- Let the following condition hold:

$$(c-a)(a-b+c)>0, \quad (8)$$

then map (7) has a discrete Lorenz-like attractor that is pseudohyperbolic for all ε from an open, adjoining to $\varepsilon=0$, subregion $\mathcal{D}$ of $\{\varepsilon_1>0, \varepsilon_1+\varepsilon_3>0, |\varepsilon_2-\varepsilon_1-\varepsilon_3| \le L(\varepsilon_1^2+\varepsilon_3^2)\}$, for some $L>0$.

Condition (8) can be considered as a simple criterion for the existence of pseudohyperbolic discrete Lorenz-like attractors in three-dimensional orientable diffeomorphisms that allow a codimension-3 bifurcation related to the appearance of a fixed (or periodic) point with the triplet $(-1,-1,+1)$ of multipliers. In particular, the inequality (8) satisfies automatically for map (1), for which $c=-1, a=0$, and $b=0$. However, for example, for the map

$$\bar{x}=y,\ \bar{y}=z,\ \bar{z}=M_1+Bx+M_2z-y^2, \quad (9)$$

which is well known as a "homoclinic map,"[59,61] where $a=-1$, $c=0, b=0$, inequality (8) is not fulfilled. In principle, this is not surprising, since map (9) is inverse to map (1), and, hence, it should have a Lorenz-like repeller (for $|B|>1$) instead of the attractor.

Note that when $B=0$ map (9) becomes effectively two-dimensional map of form $\bar{y}=z,\ \bar{z}=M_1+M_2z-y^2$. It is the well-known two-dimensional endomorphism introduced by Mirá[62] yet in 1960s. Therefore, we will call map (9) the three-dimensional Mirá map. As it was shown in Refs. 17 and 19, map (9) demonstrates chaos of completely different type than map (1)—it is more associated with spiral attractors than with Lorenz-like ones.[17,19,63,64] Nevertheless, the question of the existence of discrete Lorenz-like attractors (on periodic orbits) in map (9) is very interesting, in particular, it is important for the development of the multidimensional Newhouse theory.[39]

B. On numerical verification of pseudohyperbolicity

Let us return to the attractors presented in Figs. 1(a) and 1(b), for which we now consider the question of their pseudohyperbolicity. Note that the corresponding values of the parameters $(M_1=0, M_2=0.85, B=0.7$ and $M_1=0, M_2=0.815, B=0.7)$ are not close to $A^*=(M_1=-1/4, M_2=1, B=1)$. Thus, we cannot deduce the desired pseudohyperbolicity of these attractors from the local analysis. It is not at all clear how to establish the pseudohyperbolicity of such attractors analytically but this can be done numerically.

We will use standard tools, which, in fact, give only "numeric evidence," in contrast to the so-called "computer-assisted proofs" (see, e.g., Refs. 8, 65, 66, and 67), which give mathematical results. However, the latter are too time-consuming and require special skills. However, our approach can be viewed as an exploratory one and the results obtained can be considered as starting points for rigorous numerics. However, before doing our computations, some simple necessary conditions should be checked.

First, the fixed point itself must be pseudohyperbolic. This follows from the fact that its multipliers satisfy condition (4) in both cases of Figs. 1(a) and 1(b). Thus, if the attractors are pseudohyperbolic, then $\dim N_1=1$ and $\dim N_2=2$. This follows also that the spectrum of Lyapunov exponents $\Lambda_1>\Lambda_2>\Lambda_3$ on the attractors must be such that the inequalities

$$\Lambda_1>0,\ \Lambda_1+\Lambda_2>0,\ \Lambda_1+\Lambda_2+\Lambda_3<0 \quad (10)$$

are fulfilled.

This follows that $\Lambda_3<0$, while the sign of Λ_2 can be either positive or negative. Moreover, in Ref. 3, a mysterious behavior of the exponent Λ_2 was discovered in the case of discrete Lorenz-like attractors [the same as in Fig. 1(a) and 1(b)], for which the sign of Λ_2 was not determining reliably enough. It is quite possible that this

is well for pseudohyperbolicity, but most likely this fact does not matter much (see discussion in Ref. 3).

It is shown standardly that inequalities (10) are valid for numerically found exponents Λ_i [for both the attractors of Figs. 1(a) and 1(b)]. However, such Lyapunov exponents are certain average characteristics for the orbits of attractor; therefore, in principle, it is possible that the attractor has very small "gaps" (whose sizes may be less than any reasonable accuracy of calculations), where conditions (10) on exponents for the corresponding orbits from "gaps" are violated.

In order to exclude (as confident as possible) this situation, one can additionally check numerically conditions from Definition 1. As it seems, condition (ii) from this definition looks to be the most delicate and indicative. It says, in particular, that the field $N_1(x)$ of strongly contracting directions depends continuously on points x of the attractor. This field can be calculated in various ways. In particular, one of such methods, the so-called LMP method (abbreviation for "Light Method of Pseudohyperbolicity" checking), was proposed in Ref. 31 (see also Ref. 40). This method allows to construct a field of vectors corresponding to the strongest contractions and to display, in the form of LMP-graph, the dependence of the angles $d\varphi$ between vectors $N_1(x_1)$ and $N_1(x_2)$ on the distance dx between the corresponding points x_1 and x_2 on the attractor.

In Figs. 10(a) and 10(b), we represent the LMP-graphs for the discrete Lorenz-like attractors in Figs. 1(a) and 1(b), respectively. The graph in Fig. 10(b) shows that the corresponding attractor is pseudohyperbolic with a lot of confidence. Indeed, here $d\varphi \to 0$ as $dx \to 0$, as it should be when the field N_1 is continuous. On the other hand, the graph in Fig. 10(a) looks quite "chaotic" near the axis $dx = 0$: it seems that if $dx \to 0$, then various sequences $d\varphi = d\varphi(dx)$ can take any partial limits in $[0, \pi]$. This shows that here the condition (ii) of continuity of the field N_1 from Definition 1 is not fulfilled. The latter is characteristic for quasiattractors.

In Fig. 10(c), the LMP-graph for the attractor presented in Fig. 7(f) is shown, which can be considered as numerical evidence of the fact that this discrete Lorenz attractor of map (1) is pseudohyperbolic.

In Fig. 10(d), the LMP-graph is shown for the periodically perturbed Lorenz-like attractor presented in Fig. 2(b). This graph gives again a numerical evidence for pseudohyperbolicity of the attractor and can be considered as a certain justification of the Turaev–Shilnikov theory[16] that the pseudohyperbolicity of

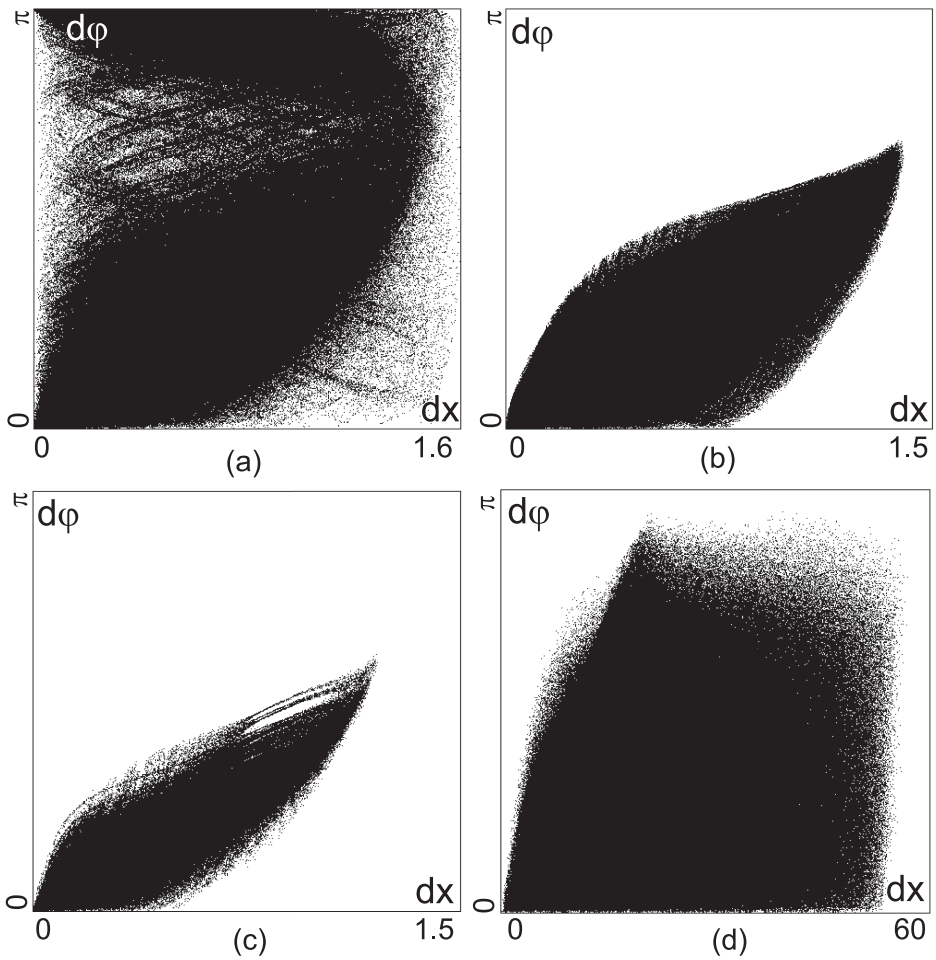

FIG. 10. LMP-graphs for the attractors presented in (a) Fig. 1(a), (b) Fig. 1(b), (c) Fig. 7(f), and (d) Fig. 2(b).

autonomous flows preserves at small periodic perturbations (see also Sec. IV D).

C. On some peculiarities of the LMP method

First, it should be noted that there is a big difference between the standard method for calculating the Lyapunov exponents and the LMP method if we only mean checking the pseudohyperbolicity. The first method is directed to the calculation of Lyapunov exponents, suppose, with huge accuracy and reliability. However, the entire phase space (a neighborhood of the attractor) cannot be scanned, in principle. Even if we try to do this, there will still be "holes" whose sizes are less than any reasonable accuracy (where, for example, periodic sinks reside), which the standard method does not feel (moreover, possible deviations in the process of calculations are leveled out due to the averaging that is the essence of the method). The LMP method works in such a way that, using all the data obtained during the calculation of Lyapunov exponents, it automatically identifies those *possible* temporary failures in the calculation of exponents.

For example, it is well known that Lyapunov exponents $\Lambda_1 > 0$ and $\Lambda_2 < 0$ in the case of the Hénon map can be calculated with high accuracy, but this does not mean at all that the attractor is hyperbolic; on the contrary, it is always a quasiattractor. In particular, in this case, there is no continuous decomposition into the spaces E_s and E_u, as this is illustrated in Fig. 11(a): here, at close points of the phase space, the vectors e_s can have completely different directions. In another case [Fig. 11(b)], a similar situation is shown, but already for the three-dimensional pseudohyperbolic case, and here the continuity of the spaces E_{ss} and E_{cu} means, in particular, that the vectors e_{ss} are close at close points (in this case, the behavior of vectors e_s and e_u on E_{cu} is not necessarily continuous, but the subspace E_{cu} spanned by these vectors is continuous).

There is one more point related to the fact that for the inverse map T^{-1} the exponent Λ_3 becomes maximal and, hence, it will be

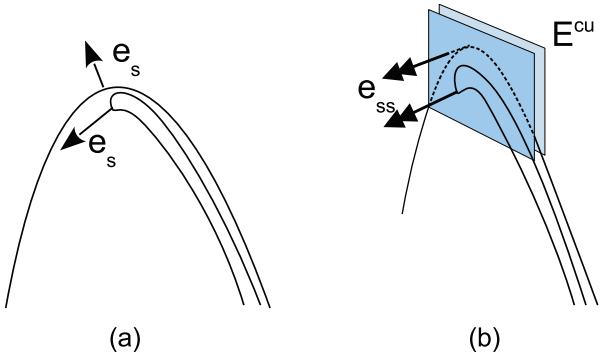

FIG. 11. Toward a (pseudo)hyperbolicity of maps: (a) in 2D Hénon-like maps, the vectors $e_s \in E_s$ can have completely different directions at close points due to strong folds in unstable invariant manifolds (the same takes place for the vectors $e_u \in E_u$); (b) in 3D maps with a pseudohyperbolic structure, strong folds in one-dimensional unstable invariant manifolds also occur, but only parallel to the planes of E^{cu} or transverse to the field of vectors from E^{ss}; therefore, vectors e_{ss} for close points will be also close.

calculated quite reliably for backward iterations, if, of course, we do not leave the attractor points. But since we have already found the array of such points during the process of calculating Lyapunov exponents, it is natural to "tie" the result of each new iteration to the corresponding point of the array.

As for questions of computational accuracy and a number of iterations, they are all standard and quite reasonable. Nevertheless, the LMP method makes it possible, for example, to distinguish between attractors in Figs. 1(a) and 1(b) with regard to their pseudohyperbolicity. So, the attractor in Fig. 1(a) turned out to be definitely a quasiattractor, while the attractor in Fig. 1(b) is pseudohyperbolic with a lot of confidence, which is demonstrated by their LMP-graphs in Figs. 10(a) and 10(b). At our request, Figueras[68] has verified our results using the computer-assisted proof method. The results are as follows: the attractor in Fig. 1(b) is indeed pseudohyperbolic; and inside the attractor of Fig. 1(a), as it turned out, there is a stable period-80 orbit whose diameter of the absorbing domain is of the order of 10^{-40}. Certainly, this is not really to obtain by means of standard numerics.

It should also be said that all the numerical results of the present paper were obtained by conventional numerical methods and do not pretend to be mathematical proofs.

D. Turaev–Shilnikov pseudohyperbolic discrete Lorenz-like attractors

One of the most natural ways to get pseudohyperbolic discrete Lorenz-like attractors for three-dimensional maps was proposed in Ref. 16 by Turaev and Shilnikov, in which it was shown that such attractors can exist in the Poincaré maps for periodically perturbed systems having the Lorenz attractor satisfying conditions of the Afraimovich–Bykov–Shilnikov model.[2] When these perturbations are sufficiently small, the resulting discrete attractor is pseudohyperbolic and has a Lorenz-like geometric structure: it contains the unique fixed point, a saddle of type (2,1), with positive multipliers, $0 < \lambda_2 < \lambda_1 < 1 < \gamma$, where $\lambda_1\gamma > 1$ and, besides, two fixed points of the Poincaré map [both saddle-foci of type (1,2)] reside in two holes of the attractor [see Fig. 2(b)]. These characteristics of such attractors make them significantly different from the discrete Lorenz-like attractors considered in Secs. II and III. Recall that the latter have fixed points with a negative unstable multiplier and period-2 points reside in two its holes.

However, for the second power of the map, these attractors may not be distinguishable at all. Nevertheless, in general, these attractors are different even in this case. In particular, the discrete Lorenz-like attractor with $\gamma < -1$ always possesses a symmetry that is inherited by the local symmetry between W^{u+} and W^{u-} due to the unstable multiplier of the fixed point O is negative. When the unstable multiplier is positive, $\gamma > 1$, the behavior of separatrices W^{u+} and W^{u-} is independent and, thus, the corresponding discrete attractor cannot be symmetric, in general. This implies also that scenarios of creation of such attractors must differ from those considered in Sec. III. Here, instead of a codimension-1 period-doubling bifurcation, one should have either a codimension-2 pitch-fork bifurcation (in the symmetric case), when the point O becomes a saddle of type (2,1) and stable fixed points p_1 and p_2 are born [see Fig. 6(b)] for the imaginary case where the points O_μ, p_1 and p_2 are fixed, or such a configuration

(two stable and one saddle fixed points) is created sharply due to a saddle-node bifurcation, when the point O remains stable and two new fixed points, saddle and stable, appear (in general, asymmetric, case).

V. ON PERIOD-2 LORENZ-LIKE ATTRACTORS

As we discussed in Sec. III for the case of three-dimensional orientable maps, good scenarios leading to the emergence of the discrete Lorenz-like attractors must contain bifurcation step [**s1**] or [**s2**]. It would seem that the same should be true for the non-orientable case as well. However, good examples of the implementation of such scenarios in the case of non-orientable maps have not yet been found (we think that their finding is only a matter of time). Instead, we found scenarios including several successive period-doubling bifurcations with the orbit (p_1, p_2). The simplest option here is as follows:

[sc3] the period-2 orbit (p_1, p_2) loses the stability under the second period-doubling bifurcation: the orbit (p_1, p_2) becomes saddle and a period-4 stable orbit $\tilde{S} = (s_1, s_2, s_3, s_4)$ is born; further, the orbit $\tilde{S}$ loses stability (under an Andronov–Hopf bifurcation) according to one of the options **[sc1]** or **[sc2]** for T^2.

Note that, *for the map* T^2, the points p_1 and p_2 become fixed and, thus, the option **[sc3]** gives a possibility for the simultaneous appearance of two discrete Lorenz-like attractors associated with these saddle fixed points. This means that, *for the map* T *itself*, a *period-2 Lorenz-like attractor* with four holes around the points s_1, s_2, s_3, s_4 can arise.

In Fig. 12, we illustrate the **[sc3]**-scenario for the nonorientable three-dimensional Hénon map (1) with fixed $B = -0.8$ and $M_2 = -1.05$, and varying M_1. When $-2.03 < M_1 < 2.172$, the fixed point O is stable. At $M_1 \approx 2.172$, it undergoes a supercritical period-doubling bifurcation and a stable period-2 orbit (p_1, p_2) becomes the attractor [Fig. 12(a)]. At $M_1 \approx 2.223$, the orbit (p_1, p_2) undergoes the second period-doubling bifurcation: it becomes saddle and a stable period-4 orbit $\tilde{S} = (s_1, s_2, s_3, s_4)$ emerges in its neighborhood [Fig. 12(b)]. A transition between Fig. 12(b) for $M_1 = 2.27$ and Fig. 12(c) for $M_1 = 2.28$ seems insignificant, but in fact, it is very important. Indeed, one can see that several events happened here:

(1) a period-4 stable invariant curve $\hat{S} = (S_1, S_2, S_3, S_4)$ is born from the stable period-4 orbit $\tilde{S}$;
(2) the most important thing is that, at some $M_1 \in (2.27; 2.28)$, a double homoclinic butterfly with the orbit (p_1, p_2) has appeared (for T^2, this means that two homoclinic butterflies with the fixed points p_1 and p_2 appear simultaneously);

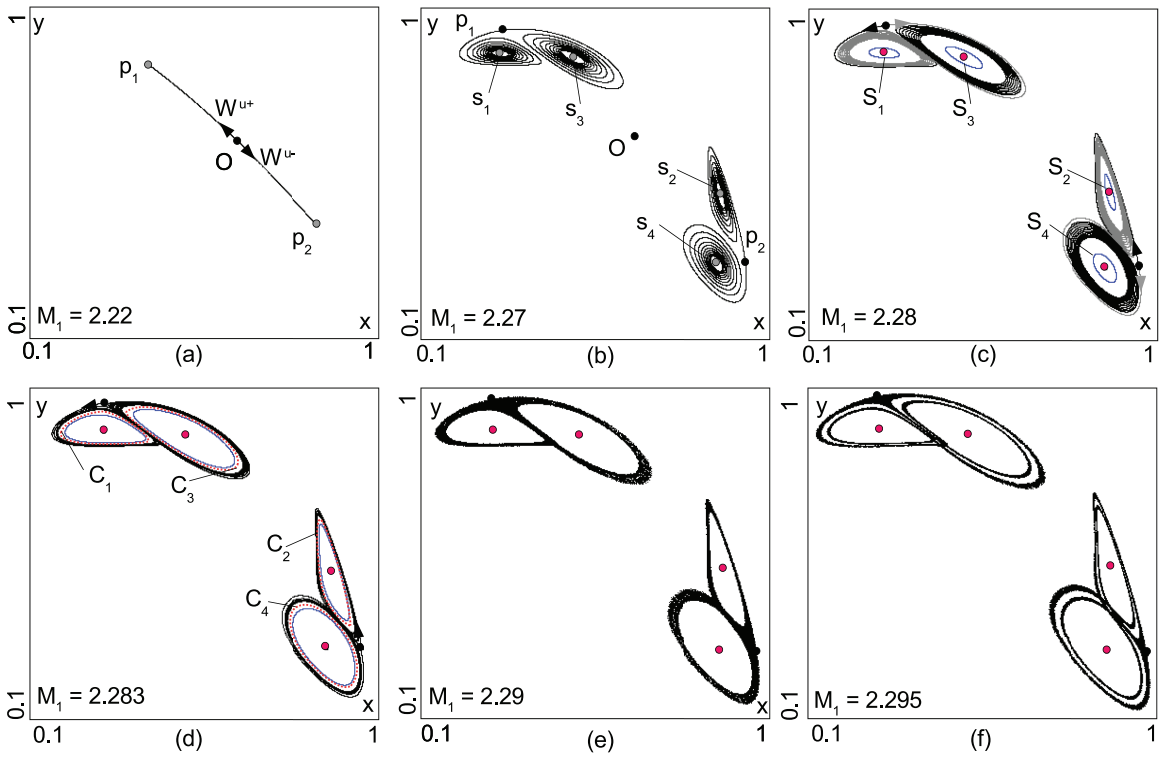

FIG. 12. Toward a scenario of the onset of a discrete period-2 Lorenz-like attractor. The upper row corresponds to simple bifurcations with fixed and period-2 points due to option **[sc3]**: (a) the fist period-doubling; (b) the secondary period-doubling; and (c) the supercritical Andronov–Hopf bifurcations. The bottom row corresponds to strange attractors that contain the points $p_1(a, b, a)$ and $p_2(b, a, b)$, where (d) $a \approx 0.29$, $b \approx 0.96$; (e) $a \approx 0.28$, $b \approx 0.97$; and (f) $a \approx 0.27$, $b \approx 0.98$.

(3) a saddle period-4 invariant curve $\hat{C} = (C_1, C_2, C_3, C_4)$ is formed from this double butterfly; the curve is saddle because the saddle value of the orbit (p_1, p_2) is greater than 1; and
(4) the unstable separatrices of points p_1 and p_2 are reconstructed (e.g., the right separatrix of p_1 goes to the point s_3 at $M_1 = 2.27$, while, at $M_1 = 2.28$, it goes to the curve S_1).

Almost immediately, the period-2 Lorenz-like attractor appears [see Fig. 12(d)] where one can see that this attractor coexists with the stable period-4 invariant curve $\hat{S}$. When the curves $\hat{S}$ and $\hat{C}$ merge and disappear, the period-2 Lorenz attractor becomes the unique attracting invariant set. Two examples of this attractor are shown in Fig. 12(e) for $M_1 = 2.29$ and Fig. 12(f) for $M_1 = 2.295$.

Note that the presented scenario for the period-2 Lorenz-like attractor is very similar to the scenario for the discrete Lorenz-like attractor in the orientable case (compare with Fig. 7). However, they are rather different attractors. Moreover, as the period-2 Lorenz-like attractor is new, in our opinion, we describe in more detail some important features of its structure and bifurcations.

So, in Fig. 13(a), a skeleton scheme for the period-2 Lorenz-like attractor is shown that is similar to the scheme from Fig. 3(b) for the discrete orientable Lorenz-like attractor. The scheme in Fig. 13(a) reflects main geometric properties of the attractor. So, the unstable manifold of the orbit (p_1, p_2) is divided by the points p_1 and p_2 into four connected components, separatrices w_1, w_2, w_3, w_4, such that $w_2 = T(w_1), w_3 = T(w_2), w_4 = T(w_3)$, and $w_1 = T(w_4)$. The local two-dimensional stable manifold of the orbit (p_1, p_2) consists also of two connected components, $W^s_{loc}(p_1)$ and $W^s_{loc}(p_2)$ that contain the points p_1 and p_2, respectively. In the case under consideration, all separatrices $w_1, \ldots, w_4$ do not intersect with $W^s(O)$ and, besides, the separatrices w_1 and w_3 intersect with $W^s(p_1)$ and do not intersect with $W^s(p_2)$, and the separatrices w_2 and w_4 intersect with $W^s(p_2)$ and do not intersect with $W^s(p_1)$.

Importantly, that the point O and its unstable manifold do not belong to the attractor, and its stable manifold forms a natural boundary between two components of the period-2 Lorenz-like attractor (or, equivalently, a boundary between two discrete Lorenz attractor for the map T^2).

The phase portrait of the period-2 Lorenz-like attractor in map (1) with $B = -0.8$, $M_1 = -1.05$, and $M_2 = 2.29$ is shown in Fig. 13(b) and behavior of its separatrix w_4 is shown in Fig. 13(d). The behavior of other separatrices, w_1, w_2, and w_3, is symmetric due to the points p_1 and p_2 compose a period-2 orbit that has the negative unstable multiplier. The latter means that $T^2(w_1) = w_3$, $T^2(w_3) = w_1$ and $T^2(w_2) = w_4$, $T^2(w_4) = w_2$.

We emphasize also that period-2 Lorenz-like attractors can be genuine (pseudohyperbolic). This applies, in particular, to the attractors in Figs. 12(d)–12(f). For example, the LMP-graph in Fig. 13(c) shows that the attractor in Fig. 13(b) [it is also in Fig. 12(e)] is certainly pseudohyperbolic.

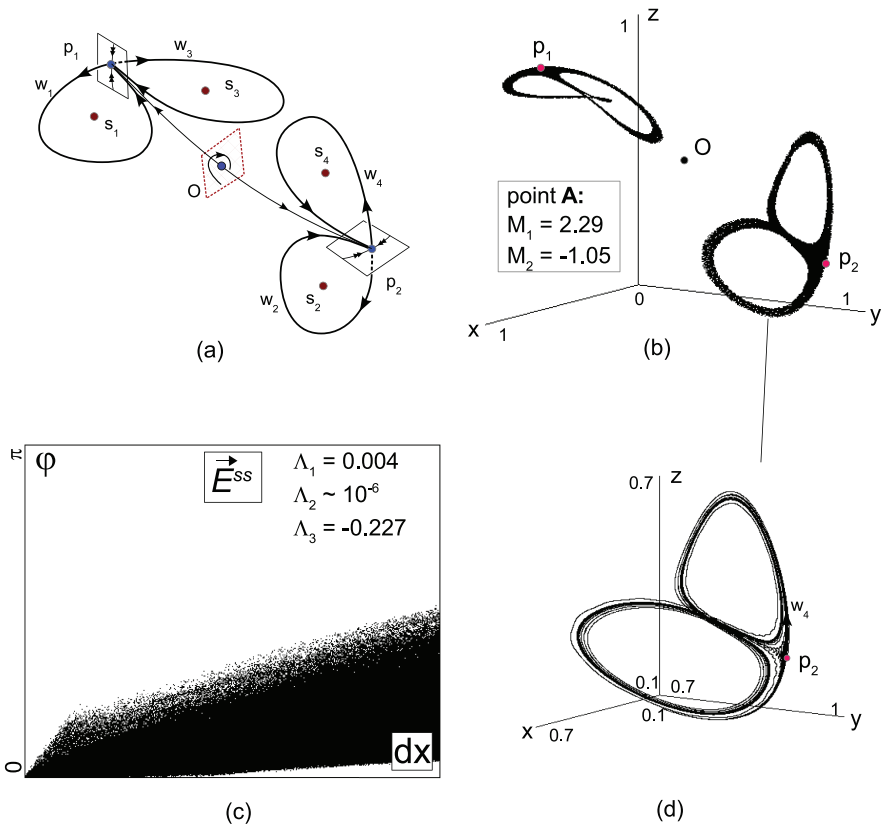

FIG. 13. Toward a structure of the period-2 Lorenz-like attractor: (a) a skeleton scheme for the unstable separatrices of points p_1, p_2, and O; (b) phase portrait for the attractor in map (1) with $B = -0.8$ $M_1 = -1.05$, and $M_2 = 2.29$; (c) its LMP-graph, and (d) numerics for its separatrix w_4. Note also that, because the period-2 Lorenz-like attractor is organized near a period-2 orbit, the LMP-graph in (c) was constructed by taking each fourth iteration of the map in order to check its pseudohyperbolicity in a proper way.

A. On crises of period-2 Lorenz-like attractors

When changing parameters, one can observe various types of crises with the period-2 Lorenz-like attractors. Usually, the same as the discrete Lorenz-like attractors,[17–19] they can break down and transform into closed invariant curves or strange attractors of torus-chaos type, etc. However, such attractors can also demonstrate their interesting features associated with the formation of strange attractors of new types.

When the unstable manifold of the orbit (p_1, p_2) begins to intersect with $W^s(O)$, it follows that new intersections of w_1 and w_3 with $W^s(p_2)$ as well as w_2 and w_4 with $W^s(p_1)$ also appear. This means that a discrete attractor can arise containing the fixed point O and the saddle period-2 orbit (p_1, p_2). A skeleton scheme for such an attractor is shown in Fig. 14(a). An example of such a discrete attractor was found in map (1) with $B = -0.8$ at $M_1 = 1.732$ and $M_2 = -0.814$ [see Fig. 14(b)]. This attractor contains the points O, p_1, and p_2 and entirely their unstable invariant manifolds that have structures like "wings." Note that the attractor contains the fixed point O with multipliers $\gamma < -1$ and $\lambda_{1,2} = \rho\, e^{\pm i\varphi}$, where $\rho \approx 0.81$ and φ is very close to $\pi/2$ ($\cos\varphi \approx 0.03$), i.e., we have a situation near the strong resonance 1:4. Thus, we also touch upon the problem of the structure of arising homoclinic attractors when passing near strong resonances, which was formulated in Ref. 17. The attractor in Fig. 14(b) is certainly the quasiattractor, since it contains the fixed point O that is a saddle-focus of type (2,1). Indirectly, this is confirmed by its LMP-graph [see Fig. 14(c)].

Remark 4.

(1) It should be noted that some interesting types of discrete spiral attractors were found in three-dimensional generalized Hénon maps near strong resonances: the so-called discrete super-spiral attractor [containing period-4 saddle-foci of both types (2,1) and (1,2)] was found in Ref. 17 nearly the strong resonance 1:4 [see Fig. 16(a)], and a discrete "triangle" spiral homoclinic attractor was found in Ref. 19 near the strong resonance 1:3 [see Fig. 16(b)].

(2) A good case of such an attractor with "wings" as in Fig. 14(c) could appear in the orientable case when the multipliers of the saddle O satisfy condition (4). In this case, the "wings" $\langle w_1, w_3\rangle$ and $\langle w_2, w_4\rangle$ should be parallel, as in the skeleton scheme in Fig. 16(c), and the attractor can be a genuine, pseudohyperbolic one. It remains only to find an example of the system (e.g., three-dimensional map) possessing such an attractor, which is an open problem.

One can imagine such a situation, when, with varying parameters, the unstable separatrices of the orbit (p_1, p_2) do no longer intersect with the stable manifold $W^s(O)$ of the fixed point O and, thus, a heteroclinic period-2 attractor is created. It contains the period-2 orbit (p_1, p_2) but does not capture the fixed point O. A skeleton scheme of such an attractor is shown in Fig. 15(a), it illustrates the main feature of the attractor related to the fact that all stable and unstable invariant manifolds of the points p_1 and p_2 mutually intersect. An example of such attractor for map (1) with $B = -0.8$ is shown in Fig. 15(b). However, we note that the first example of such attractor was found yet in Ref. 3 [see Fig. 1(d)]. However, now we understand better both its structure and how it can appear at reconstructions with the period-2 Lorenz attractors.

It is also important that such period-2 heteroclinic attractor can be pseudohyperbolic. In the case of the attractor in Fig. 15(b), its LMP-graph, shown in Fig. 15(c), confirms this fact. This graph, the same as the LMP-graph of Fig. 14, has been constructed for T^4; however, unlike the latter, it contains the point $(0, \pi)$. This does not contradict the pseudohyperbolicity of the attractor, since the points p_1 and p_2 (fixed for T^4) together with their invariant manifolds form heteroclinic cycles of non-orientable type when passing along which the initial vector can change its direction to the opposite. In particular, this concerns vectors from the invariant spaces $N_1(x)$ from Definition 1. In Fig. 15(a), we illustrate this fact by showing seven successive positions of the vectors from N_1 near the contour $[p_2, w_3, p_1, w_2]$, while the corresponding areas from N_2 are lined up in the form of Möbius band.

In order to trace better interrelations between the discrete attractors of these three types, the period-2 Lorenz attractor, the homoclinic attractor (containing the fixed point O and the period-2 orbit), and the period-2 heteroclinic attractor, we have constructed the so-called chart of Lyapunov exponents (see Fig. 17), for map (1)

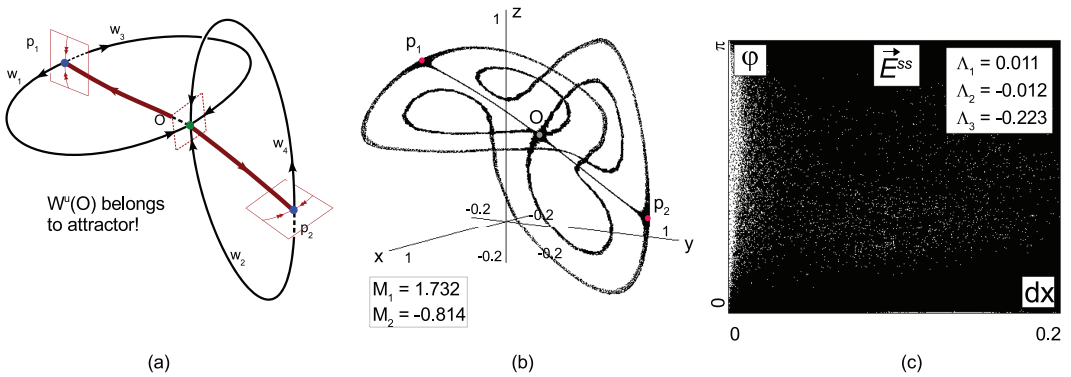

FIG. 14. Toward an attractor containing the fixed point O (that is a saddle-focus near the 1:4 resonance) and the saddle period-2 orbit (p_1, p_2): (a) a skeleton scheme for such attractors; (b) an example of such attractor in map (1) with $B = -0.8$, where $O(x = y = z \approx 0.55)$; and (c) its LMP-graph.

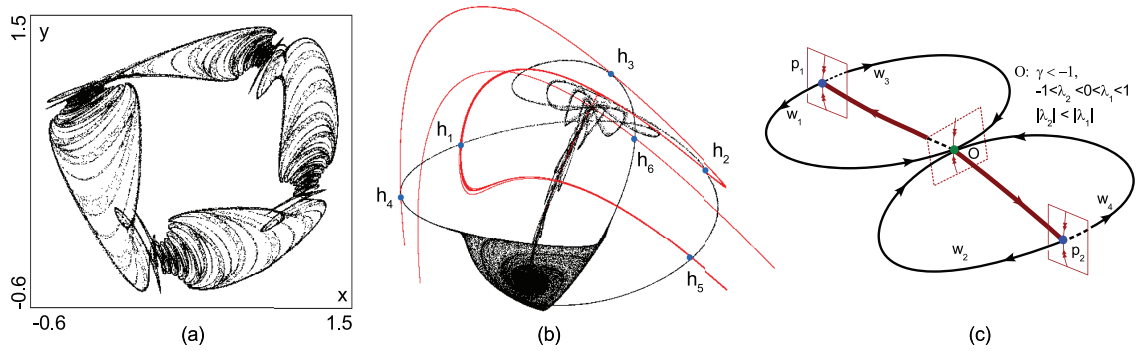

FIG. 15. (a) An example of a discrete super-spiral attractor [in map (9) with $B = 0.7$, $M_1 = 0.35$, and $M_2 = 0.8$; some point of attractor $(x, y, z) = (0.58, 1.05, 0.54)$]; (b) an example of a discrete "triangle" spiral homoclinic attractor [in map (9) with $B = 0.7$, $M_1 = 0.2185$, $M_2 = -0.1324$]; some homoclinic points, $h_1, \ldots, h_6$ are shown, where the stable (red line) and unstable manifolds of the fixed point $O = (0.3, 0.3, 0.3)$ intersect; and (c) a skeleton scheme for a genuine two-wings attractor.

with $B = -0.8$. This chart is a specific diagram, on the (M_1, M_2)-parameter plane, showing various types of stable regimes.

The blue and green domains in the chart relate to stable periodic and quasiperiodic orbits, respectively. Strange attractors exist for the values of parameters corresponding to the gray and yellow domains, which are distinguished by the magnitude of the second Lyapunov exponent Λ_2 (in the yellow-colored domain $\Lambda_2 < 0$ while in the gray-colored – Λ_2 oscillates near zero). In these domains, we mark three points A, B, and C related to the attractors presented in Figs. 13–15, respectively.

Even a quick glance at the diagram in Fig. 17 is enough to understand that the transitions between different attractors corresponding to the points A, B, and C cannot be too simple. In any case, they are associated not only with the described above reconstructions of unstable manifolds but also with the destruction of attractors themselves, their transformations into invariant curves, inverse rearrangements of these curves into new attractors, etc. Understanding the corresponding bifurcation mechanisms even in the particular case of map (1) looks potentially as a new rather interesting problem. In the present paper, we have considered, in fact, only one such mechanism—the scenario of the appearance of the period-2 Lorenz attractor due to the option **[sc3]** that is observed along the pathway marked by the turquoise arrow in Fig. 17.

VI. CONCLUSION

Discrete homoclinic attractors of multidimensional maps compose a very interesting class of new strange attractors that can be genuine, pseudohyperbolic, attractors. The theory of such attractors has not been created yet, although some important results in this direction were obtained (see, e.g., Refs. 3 and 17–19). The greatest advances in this theory have been achieved at the study of discrete Lorenz-like attractors. In the present paper, we tried to give some overview of the main results obtained in this direction. However, as one can see, even here, there are still many unsolved problems. For example, one can emphasize the following problems related to the study of the generalized Hénon maps of form (2).

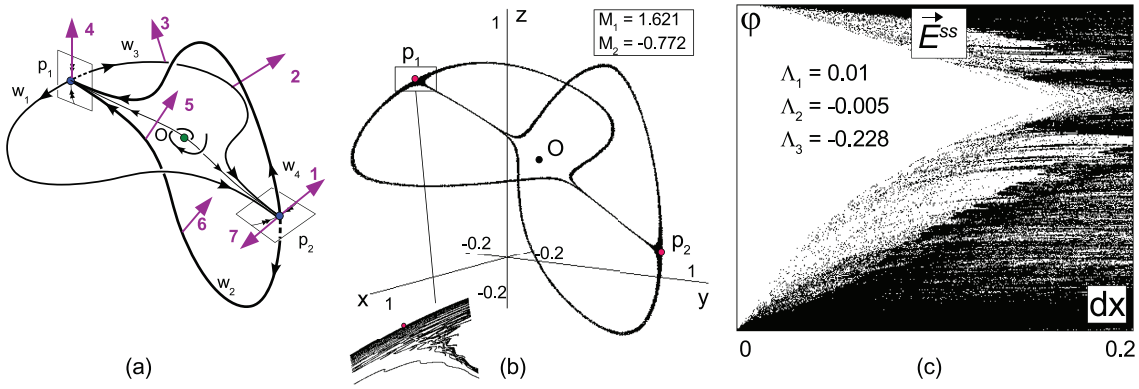

FIG. 16. Toward a period-2 heteroclinic attractor containing the saddle orbit (p_1, p_2): (a) a skeleton scheme for such attractors; (b) an example of such attractor in map (1) with $B = -0.8$, where $p_1 = (a, b, a)$, $p_2 = (b, a, b)$, and $a = 0.12$, $b = 0.85$; and (c) its LMP-graph.

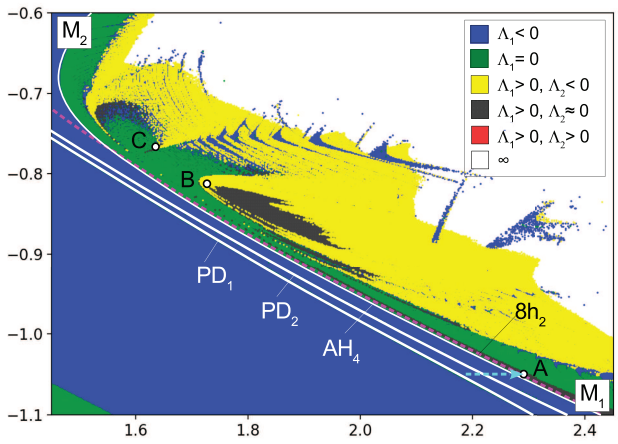

FIG. 17. Chart of Lyapunov exponents for map (1) with $B = -0.8$ on the (M_1, M_2)-parameter plane. At each of the 500 × 500 points, we compute 10 000 preliminary iterations and then estimate the first two exponents $\Lambda_1 > \Lambda_2$ over the next 100 000 iterations. The color scheme is described in a palette (see the top-right corner of this chart); the red domains (with hyperchaos) are absent in the chart. The threshold of zero LE is 0.005. Some bifurcation curves are also shown here: the curves PD_1 and PD_2 of the first and second period-doubling with the fixed point O; the curve AH_4 of the supercritical Andronov–Hopf bifurcation with the stable period-4 orbit (s_1, s_2, s_3, s_4); and the curve (a thinking zone indeed) $8h_2$ corresponding to the appearance of a double homoclinic butterfly with the orbit (p_1, p_2).

(1) To find an example of a discrete Lorenz-like attractor containing a saddle fixed point with positive multipliers (the same one as in Ref. 16).
(2) In the nonorientable case ($B < 0$), to find an example of discrete Lorenz-like attractor with fixed point, which would be pseudo-hyperbolic or would appear in the scenarios with options **[sc1]** or **[sc2]** (see Sec. II).
(3) To study local codimension-3 bifurcations of fixed points with multipliers $(+1, +1, -1)$ and/or $(-i, +i, -1)$ with the accent to the birth of discrete Lorenz-like attractors or strange attractors of other types (which ones?).
(4) To find an example of discrete Lorenz-like attractor with a saddle periodic orbit in the three-dimensional Mirá map of the form (9).

On the other hand, as we know, the zoo of discrete homoclinic attractors even in three-dimensional maps now contains several specimens, interesting from different points of view. These are, for example, a series of figure-8 attractors, including double and super figure-8 ones, as well as figure-8 spiral attractors (see Ref. 20). As for discrete Lorenz-type attractors, some of their types, predicted by their primary homoclinic structures, have not yet been found. These are, e.g., mentioned in Sec. IV D, "classical" attractors [containing a saddle fixed point of type (2,1) with all positive multipliers] or nonorientable "double Lorenz" attractors [containing a saddle fixed point of type (2,1) with multipliers $\gamma > 1, -1 < \lambda_2 < 0 < \lambda_1 < 1$].[46] A very interesting class consists of the so-called discrete Shilnikov attractors, i.e., homoclinic attractors containing a saddle-focus fixed point of type (1,2). Since such attractors contain the closure of two-dimensional unstable manifold of a fixed point, they can provide quite realistic and simple examples of hyperchaotic attractors.[44,45] Although a number of rather interesting results have already been obtained in the theory of discrete Shilnikov attractors (see, e.g., Refs. 17, 19, and 20), there is still much to be done here.

Another interesting problem can be formulated as a continuation of the topics outlined in Sec. V of this paper. In particular, for generalizing options **[sc1]**, **[sc2]**, and **[sc3]**, we consider the following:

[$\mathbf{sc}_n$] the fixed point O undergoes n supercritical period-doubling bifurcations and this sequence is terminated by the Andronov–Hopf bifurcation, i.e., the stable orbit of period 2^n loses stability according to the options [s1] or [s2] for T^{2n}.

As a result of this option, a period-2^n Lorenz-like attractor can theoretically appear. Next, components of this attractor can merge pairwise forming a 2^{n-1}-component attractor containing period-2^n points and organizing them (after period-doubling) period-2^{n-1} points, etc.

This option implies that, in principle, the following sequence of attractor crises can be observed: a period-2^n Lorenz-like attractor appears $\Rightarrow$ 2^n components of this attractor merge in pairs forming 2^{n-1}-component attractor $\Rightarrow \cdots \Rightarrow$ a homoclinic (of Lorenz shape or not) attractor containing the fixed point O appears. This sequence of attractor crises can be viewed as a "chain of doublings of discrete Lorenz shape attractors." In this paper, we have only slightly touched on this topic using the example of such a chain with $n = 1$. Of course, the question on such chains with larger values of n seems rather interesting, and we plan to consider this problem in more detail in the nearest future.

ACKNOWLEDGMENTS

The authors thank D. Turaev and P. Kuptsov for fruitful discussions and useful remarks. This paper was carried out in the framework of the RSciF under Grant Nos. 19-11-00280 (Secs. I, V, and VI) and 17-11-01041 (Secs. II and III) and also by RFBR under Grants Nos. 19-01-00607 (Secs. IV A and IV D) and 18-29-10081 (Sec. IV C). The authors were also partially supported (numerical experiments in Secs. III, IV B, and V) by Laboratory of Dynamical Systems and Applications NRU HSE, of the Ministry of Science and Higher Education of the RF under Grant No. 075-15-2019-1931. S.G., A.K., and E.S. acknowledge the Theoretical Physics and Mathematics Advancement Foundation "BASIS" for support in scientific investigations.

DATA AVAILABILITY

The data that support the findings of this study are available from the corresponding author upon reasonable request.

REFERENCES

[1]V. Afraimovich, V. Bykov, and L. Silnikov, "The origin and structure of the Lorenz attractor," Dokl. Akad. Nauk SSSR **234**, 336–339 (1977).
[2]V. Afraimovich, V. Bykov, and L. Shilnikov, "On attracting structurally unstable limit sets of Lorenz attractor type," Trudy Moskov. Mat. Obshch. **44**, 150–212 (1982).

[3]S. V. Gonchenko, I. I. Ovsyannikov, C. Simó, and D. V. Turaev, "Three-dimensional Hénon-like maps and wild Lorenz-like attractors," Int. J. Bifurcat. Chaos **15**, 3493–3508 (2005).
[4]E. N. Lorenz, "Deterministic nonperiodic flow," J. Atmos. Sci. **20**, 130–141 (1963).
[5]J. Guckenheimer and R. F. Williams, "Structural stability of Lorenz attractors," Publ. Math. Inst. Hautes Études Sci. **50**, 59–72 (1979).
[6]L. Shilnikov, "The bifurcation theory and quasi-hyperbolic attractors," Usp. Mat. Nauk **36**, 240–241 (1981).
[7]A. Shilnikov, L. Shilnikov, and D. Turaev, "Normal forms and Lorenz attractors," Int. J. Bifurcat. Chaos **3**, 1123–1139 (1993).
[8]W. Tucker, "The Lorenz attractor exists," C. R. Acad. Sci. Ser. I Math. **328**, 1197–1202 (1999).
[9]I. Ovsyannikov and D. Turaev, "Analytic proof of the existence of the Lorenz attractor in the extended Lorenz model," Nonlinearity **30**, 115 (2016).
[10]M. Hénon, "A two-dimensional mapping with a strange attractor," in *The Theory of Chaotic Attractors* (Springer, 1976), pp. 94–102.
[11]C. Simó, "On the Hénon-Pomeau attractor," J. Stat. Phys. **21**, 465–494 (1979).
[12]P. Cvitanović, G. H. Gunaratne, and I. Procaccia, "Topological and metric properties of Hénon-type strange attractors," Phys. Rev. A **38**, 1503 (1988).
[13]M. Benedicks and L. Carleson, "The dynamics of the Hénon map," Ann. Math. **133**, 73–169 (1991).
[14]R. Ures, "On the approximation of Hénon-like attractors by homoclinic tangencies," Ergod. Theory Dyn. Syst. **15**, 1223–1229 (1995).
[15]R. Vitolo, "Bifurcations of attractors in 3D diffeomorphisms," Ph.D. thesis (University of Groningen, 2003).
[16]D. Turaev and L. Shilnikov, "Pseudohyperbolicity and the problem on periodic perturbations of Lorenz-type attractors," in *Doklady Mathematics* (Pleiades Publishing, 2008), Vol. 77, p. 17.
[17]S. V. Gonchenko, A. S. Gonchenko, and L. P. Shilnikov, "Towards scenarios of chaos appearance in three-dimensional maps," Russ. J. Nonlinear Dyn. **8**, 3–28 (2012).
[18]S. Gonchenko, A. Gonchenko, I. Ovsyannikov, and D. Turaev, "Examples of Lorenz-like attractors in Hénon-like maps," Math. Model. Nat. Phenom. **8**, 48–70 (2013).
[19]A. Gonchenko, S. Gonchenko, A. Kazakov, and D. Turaev, "Simple scenarios of onset of chaos in three-dimensional maps," Int. J. Bifurcat. Chaos **24**, 1440005 (2014).
[20]A. Gonchenko and S. Gonchenko, "Variety of strange pseudohyperbolic attractors in three-dimensional generalized Hénon maps," Physica D **337**, 43–57 (2016).
[21]S. Gonchenko, C. Simó, and A. Vieiro, "Richness of dynamics and global bifurcations in systems with a homoclinic figure-eight," Nonlinearity **26**, 621 (2013).
[22]M. Malkin, "Rotation intervals and the dynamics of Lorenz type mappings," Selecta Mathematica Sovietica **10**(3), 265–275 (1991).
[23]M.-C. Li and M. Malkin, "Smooth symmetric and Lorenz models for unimodal maps," Int. J. Bifurcat. Chaos **13**, 3353–3371 (2003).
[24]L. Shilnikov, "Bifurcation theory and the Lorenz model," in *The Hopf Bifurcation and Its Applications*, Appendix to Russian ed., edited by J. Marsden and M. McCraken (M.: Mir, 1980), pp. 317–335.
[25]A. S. Gonchenko, S. V. Gonchenko, and A. O. Kazakov, "Richness of chaotic dynamics in nonholonomic models of a Celtic stone," Regul. Chaotic Dyn. **18**, 521–538 (2013).
[26]J. Eilertsen and J. Magnan, "On the chaotic dynamics associated with the center manifold equations of double-diffusive convection near a codimension-four bifurcation point at moderate thermal Rayleigh number," Int. J. Bifurcat. Chaos **28**, 1850094 (2018).
[27]J. S. Eilertsen and J. F. Magnan, "Asymptotically exact codimension-four dynamics and bifurcations in two-dimensional thermosolutal convection at high thermal Rayleigh number: Chaos from a quasi-periodic homoclinic explosion and quasi-periodic intermittency," Physica D **382**, 1–21 (2018).
[28]C. A. Morales, M. J. Pacífico, and E. R. Pujals, "On C^1 robust singular transitive sets for three-dimensional flows," C. R. Acad. Sci. Ser. I Math. **326**, 81–86 (1998).
[29]E. A. Sataev, "Some properties of singular hyperbolic attractors," Sbornik Math. **200**, 35 (2009).
[30]D. V. Turaev and L. P. Shilnikov, "An example of a wild strange attractor," Sbornik Math. **189**, 291 (1998).
[31]S. Gonchenko, A. Kazakov, and D. Turaev, "Wild spiral attractors in a four-dimensional Lorenz model," Nonlinearity **34**, 2 (2021).
[32]S. Newhouse, "Non-density of axiom A(a) on S^2, global analysis," in *Proceedings of Symposia in Pure Mathematics* (AMS, 1968), Vol. 14, pp. 191–202.
[33]S. E. Newhouse, "The abundance of wild hyperbolic sets and non-smooth stable sets for diffeomorphisms," Publ. Math. IHÉS **50**, 101–151 (1979).
[34]S. Gonchenko, D. Turaev, and L. Shilnikov, "On an existence of Newhouse regions near systems with non-rough Poincaré homoclinic curve (multidimensional case)," in *Doklady Akademii Nauk* (Pleiades Publishing, 1993), Vol. 329, pp. 404–407.
[35]J. Palis and M. Viana, "High dimension diffeomorphisms displaying infinitely many periodic attractors," Ann. Math. **140**, 207–250 (1994).
[36]N. Romero, "Persistence of homoclinic tangencies in higher dimensions," Ergod. Theory Dyn. Syst. **15**, 735–757 (1995).
[37]S. Gonchenko, L. Shilnikov, and D. Turaev, "On models with non-rough Poincaré homoclinic curves," Physica D **62**, 1–14 (1993).
[38]S. Gonchenko, D. Turaev, and L. Shilnikov, "Homoclinic tangencies of arbitrarily high orders in the Newhouse regions," Contemp. Math. Appl. **67**, 69–128 (1999).
[39]S. V. Gonchenko, L. P. Shilnikov, and D. V. Turaev, "On dynamical properties of multidimensional diffeomorphisms from Newhouse regions: I," Nonlinearity **21**, 923 (2008).
[40]A. S. Gonchenko, S. V. Gonchenko, A. O. Kazakov, and A. D. Kozlov, "Elements of contemporary theory of dynamical chaos: A tutorial. Part I. Pseudohyperbolic attractors," Int. J. Bifurcat. Chaos **28**, 1830036 (2018).
[41]A. V. Borisov, A. O. Kazakov, and I. R. Sataev, "Spiral chaos in the nonholonomic model of a Chaplygin top," Regul. Chaotic Dyn. **21**, 939–954 (2016).
[42]E. A. Grines, A. O. Kazakov, and I. R. Sataev, "Discrete Shilnikov attractor and chaotic dynamics in the system of five identical globally coupled phase oscillators with biharmonic coupling," arXiv:1712.03839 (2017).
[43]S. V. Gonchenko, A. S. Gonchenko, A. O. Kazakov, A. D. Kozlov, and Y. V. Bakhanova, "Mathematical theory of dynamical chaos and its applications: Review. Part 2. Spiral chaos of three-dimensional flows," Izv. VUZ. Appl. Nonlinear Dyn. **27**, 7–52 (2019).
[44]I. R. Garashchuk, D. I. Sinelshchikov, A. O. Kazakov, and N. A. Kudryashov, "Hyperchaos and multistability in the model of two interacting microbubble contrast agents," Chaos **29**, 063131 (2019).
[45]N. Stankevich, A. Kazakov, and S. Gonchenko, "Scenarios of hyperchaos occurrence in 4D Rössler system," Chaos **30**, 123129 (2020).
[46]A. Gonchenko, M. Gonchenko, and E. Samylina, "On scenarios of chaos onset in three-dimensional nonorientable maps," Chaos (in press) (2021).
[47]A. V. Borisov, A. O. Kazakov, and I. R. Sataev, "The reversal and chaotic attractor in the nonholonomic model of Chaplygin's top," Regul. Chaotic Dyn. **19**, 718–733 (2014).
[48]A. L. Shilnikov, "Bifurcation and chaos in the Morioka–Shimizu system," Methods Qual. Theory Differ. Equ. **180193**, 105–117 (1986).
[49]A. Chenciner and G. Iooss, "Bifurcations de tores invariants," Arch. Ration. Mech. Anal. **69**, 109–198 (1979).
[50]A. Gonchenko and E. Samylina, "On the region of existence of a discrete Lorenz attractor in the nonholonomic model of a Celtic stone," Radiophys. Quantum Electron. **62**, 369–384 (2019).
[51]V. S. Afraimovich and L. P. Shilnikov, "On small periodic perturbations of autonomous systems," in *Doklady Akademii Nauk* (Pleiades Publishing, 1974), Vol. 214, pp. 739–742.
[52]A. Shilnikov, "Bifurcation and chaos in the Morioka–Shimizu system," Methods Qual. Theory Differ. Equ. Gorky **180193**, 105–117 (1986).
[53]A. L. Shilnikov, "On bifurcations of the Lorenz attractor in the Shimizu–Morioka model," Physica D **62**, 338–346 (1993).
[54]V. Afraimovich and L. P. Shilnikov, "Invariant two-dimensional tori, their breakdown and stochasticity," Am. Math. Soc. Transl. **149**, 201–212 (1991).

[55]V. Afraimovich and L. Shilnikov, "Strange attractors and quasiattractors," in *Nonlinear Dynamics and Turbulence* (1983), pp. 1–28.
[56]N. Gavrilov and L. Shilnikov, "On three-dimensional dynamical systems close to systems with a structurally unstable homoclinic curve. I," Math. USSR Sbornik **17**, 467 (1972).
[57]S. Gonchenko, "On stable periodic motions in systems that are close to systems with a structurally unstable homoclinic curve," Mat. Zametki **33**, 745–755 (1983).
[58]S. Gonchenko, L. Shilnikov, and D. Turaev, "Quasiattractors and homoclinic tangencies," Comput. Math. Appl. **34**, 195–227 (1997).
[59]S. V. Gonchenko, D. V. Turaev, and L. P. Shilnikov, "Dynamical phenomena in multidimensional systems with a structurally unstable homoclinic Poincaré curve," Dokl. Akad. Nauk **330**, 144–147 (1993).
[60]S. Kuznetsov, *Dynamical Chaos and Hyperbolic Attractors: From Mathematics to Physics* (Institute of Computer Research, Izhevsk, Moscow, 2013).
[61]S. V. Gonchenko, A. S. Gonchenko, and L. P. Shilnikov, "On a homoclinic origin of Hénon-like maps," Regul. Chaotic Dyn. **15**, 462–481 (2010).
[62]C. Mira, "Determination pratique du domaine de stabilite d'un point d'equilibre d'une recurrence non iineaire du deuxieme ordre a variables reelies, C," C. R. Acad. Sci. Paris Ser. A, 5314–5317 (1965).
[63]A. Shykhmamedov, E. Karatetskaia, A. Kazakov, and N. Stankevich, "Hyperchaotic attractors of three-dimensional maps and scenarios of their appearance," arXiv:2012.05099 (2020).
[64]E. Karatetskaia, A. Shykhmamedov, and A. Kazakov, "Shilnikov attractors in three-dimensional orientation-reversing maps," Chaos **31**, 011102 (2021).
[65]W. Tucker, "A rigorous ode solver and Smale's 14th problem," Found. Comput. Math. **2**, 53–117 (2002).
[66]M. J. Capinski and A. Wasieczko-Zajac, "Computer-assisted proof of Shil'nikov homoclinics: With application to the Lorenz-84 model," SIAM J. Appl. Dyn. Syst. **16**, 1453–1473 (2017).
[67]M. J. Capiński, D. Turaev, and P. Zgliczyński, "Computer assisted proof of the existence of the Lorenz attractor in the Shimizu–Morioka system," Nonlinearity **31**, 5410 (2018).
[68]J. L. Figueras, private communication (2016).